Annual Progress Report

ULI2 Step-B-0060, Composite Manufacturing Technologies for Aerospace Performance at Automotive Production Rates

Grant Number 80NSSC20M0164

Principal Investigator
John W. Gillespie Jr.
Center for Composite Materials
101 Academy Street
Newark, DE 19716

September 1, 2022– August 31, 2023

NASA Technical Points of Contact
Koushik Datta, Koushik.Datta@nasa.gov
Dawn C. Jegley, dawn.c.jegley@nasa.gov

Report submitted to:
Technical Officer / Koushik Datta
NASA Ames Research Center
Moffett Field, CA 94035-1000

Grants Officer
NASA Shared Services Center
Procurement Office, Bldg 1111
Stennis Space Center, MS 39529
NSSC-Grant-Report@mail.nasa.gov

New Technology Representative
NASA Ames Research Center
Code 202A-3
Moffett Field, CA 94035-1000
kelly.l.garcia@nasa.gov

TABLE of CONTENTS

Executive Summary

The National Aeronautics and Space Administration (NASA) University Leadership Initiative selected a team led by the University of Delaware Center for Composite Materials (UD-CCM) to address technology barriers and education/workforce training needs in composites manufacturing technologies providing aerospace performance at automotive production rates for the Urban Air Mobility (UAM) and commercial air platforms. Our program is a 4-year effort. This Annual Progress report covers the third year of the program from September 1, 2022, to August 31, 2023. The annual report includes a summary of program highlights in the areas of research and education/workforce training.

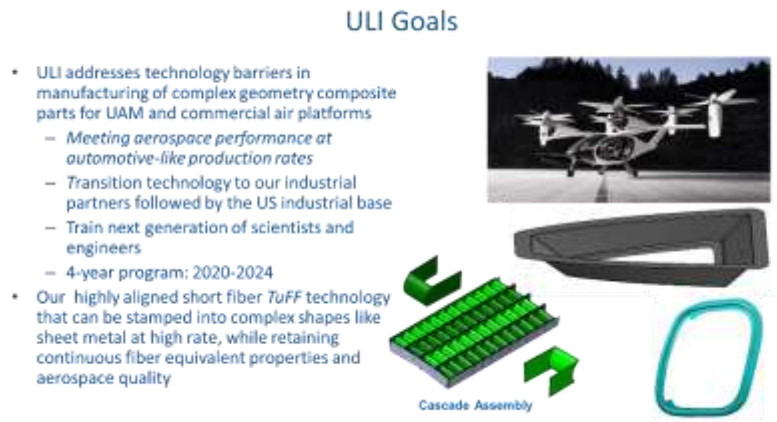

Our Team

Our team consists of UD-CCM as the lead organization with core team members from the composite supply chain from material suppliers, part manufacturers (ATC, David Leach), and UAM and aerospace system integrators (Joby Aviation, John Geriguis & Spirit AeroSystems, Kerrick Dando). Our academic partner is Southern University (SU PI is Professor Patrick Mensah) who is actively involved in research and contributing to our education and outreach activities to underrepresented minorities from K-14 in aerospace applications of composites. Our outreach to other institutions is significant and include other academic and commercial entities.

Background on NASA Grand Challenge for UAM

Urban Air Mobility (UAM), a safe and efficient air transportation system for on-demand mobility (ODM) from small package delivery to air taxis, has arrived as the next frontier in air transportation. With NASA leading UAM efforts in identifying technical, operational challenges and regulatory frameworks, a community of small to large companies are investing significant resources into establishing infrastructure, digital frameworks, platforms, and operational models. Market studies[1] have established economic factors (estimated market size ~$500B, projected total number of air taxis exceed 850,000 in the US alone) with NASA setting forth a Grand Challenge. With higher production volumes and smaller size than commercial aircraft, studies have identified the need for next generation composite materials and manufacturing methods to meet ODM goals of affordability, safety, and lifecycle emissions. However, the maturity levels of today's manufacturing readiness[2] to achieve aerospace performance at automotive rates is ranked low. A NASA Roadmap in manufacturing and integrated structures[3] identified UAM technology for a 15-year timeframe with operational prototypes by 2026, and technology scaling by 2031. Flexible automated composite manufacturing methods were identified, in combination with integrated structure/material concepts for anti-ice, health monitoring etc. Similarly, commercial air platforms have made the change to composites use for large structures (wings, fuselage etc.), but retain metal components for smaller, complex parts typical of the UAM vehicles.

Our Approach

Our project addresses these technology barriers in manufacturing of complex geometry composite parts for UAM and commercial air platforms by use our revolutionary highly aligned short fiber technology (called *TuFF* or Tailorable universal Feedstock for Forming) that can be formed into complex shapes like sheet metal at high rate, while retaining continuous fiber equivalent properties and aerospace quality. The novel material and manufacturing approach create a paradigm shift for manufacturing of commercial air and UAM vehicle structures.

Under a 4-year DARPA-funded program (2017-2021) and an Office of Naval Research Defense University Research Instrumentation Program (ONR DURIP) Equipment Grant, UD-CCM has developed a pilot that aligns short fiber into preforms, creates prepreg by film infusion and includes a forming cell to produce formed parts at rate in one facility. This equipment is being used in our ULI program to make materials for all ULI research tasks as well as for forming trials on aerospace parts identified by our team members. The site will also be used for training of Historically black colleges and universities (HBCU) faculty and students from Southern University and to facilitate technology transition for the UAM and aerospace supply chain.

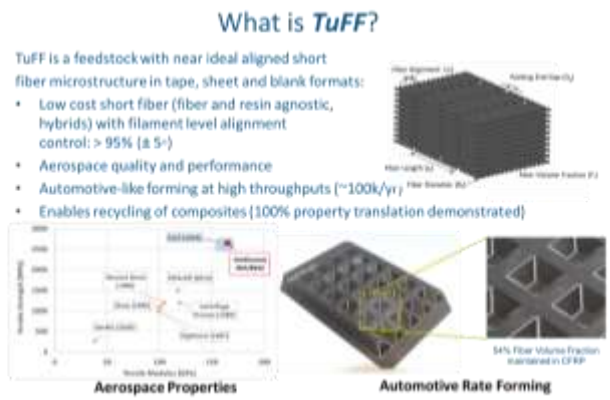

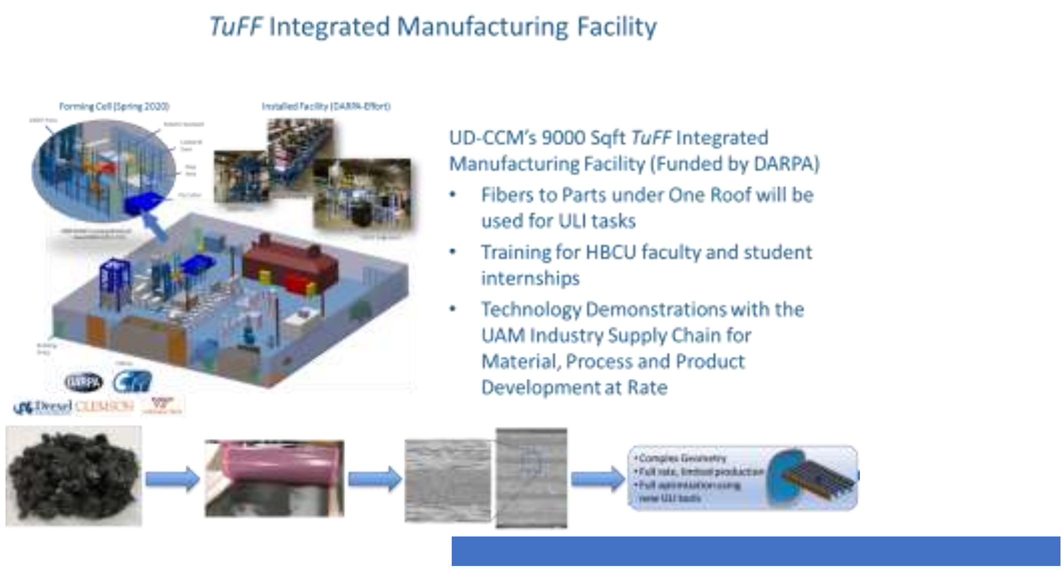

Our TuFF pilot-scale facility allows part manufacturing from short fibers under one roof

ULI Advisory Board and Meetings

An External Advisory Board (EAC) has been established to evaluate our ULI program progress. The chair of the Board is Mr. Mick Maher with over 30 years of experience in composites as former Program Director at Defense Advanced Research Projects Agency (DARPA) who ran the Open Manufacturing and Tailored Feedstock for Forming composite aerospace initiatives, Branch Chief of the Composites Branch at Army Research Lab (ARL) and worked in the composites industry for decades. He has recruited board member from industry original equipment manufacturers (OEM) and the supply chain, academia, and the FAA. The board convenes during our annual program review (first year review was held on 10/20/21; second year review was held on 10/13/22 and third year review is scheduled for 10/26/23). Annual reports are also provided to EAC members prior to annual reviews. We have created a public website for our ULI (https://www.ccm.udel.edu/research/program-highlights/nasa-university-leadership-initiative-uli/) where all past presentations, reports, publications and other activities are posted and can be accessed throughout the year.

ULI External Advisory Board

Board Chair: Michael Maher

Industry OEMs

- Spirit: Kim Caldwell
- Joby: John Geriguis

Academia

- Prof. Shridhar Yarlagadda (UD-CCM)
- Prof. Srikanth Pilla (Clemson)
- Prof. Jim Sherwood (UMass)

FAA: Curt Davies

Advisory Board Feedback

- The EAC commends the attention UDel paid to addressing comments form last year's meeting.
- Having the industry partners brief plans for specific application/demos using TuFF material format and active participation in the review was well received by the committee.
- The program is doing an excellent job of understanding the fundamental behavior of the TuFF material. The modeling and characterization work is very strong.
- A clearer roadmap for technology adoption would be beneficial.
- The committee was pleased with the described workforce development program and the collaboration between UDel and Southern.
- It would be helpful that when making comparison of properties that the variables between materials/classes be minimized.
- It's not clear how much the industry partners' manufacturing experience is influencing the forming development.
- The committee was happy to see SU student working at CCM. We strongly encourage this collaboration be strengthened as well as more integrated with the main TuFF program.
- As a follow-up to our meeting at the review, the committee found the tours that followed to be very impressive. Seeing the process helped provide context to the technical program being executed.

In terms of meetings, we have weekly internal meeting with task leads, monthly meetings with our external team members, monthly technical meetings with NASA (organized by Dawn Jegley and Kaushik Datta) and annual meetings with our external board.

Highlights of October 2022 Annual Meeting

Participation:

- 195 Registered Attendees
  - 126 Online
    - 117 – External academic and industry
  - 39 In-Person
    - 27 – External academic and industry

NASA ULI Website:

In November we created the NASA ULI webpages within the UD-CCM website to provide easier access to program information.

Visit - *https://www.ccm.udel.edu/research/program-highlights/nasa-university-leadership-initiative-uli/*

Education, Workforce, Outreach and Diversity Highlights

UD-CCM and Southern University were actively involved in education/workforce training and outreach during the past year. More than 2,500 students were involved with approximately 1700 underrepresented minorities from Baton Rouge LA. The highlights include:

1) Internship Recruitment for NASA Research Centers: 19 students applied to 7 NASA sites; 2 ULI internships at NASA Langley.

Eli Bogetti
University of Delaware
Masters in Mechanical Engineering
Data Science, December 2023

Alexander Barry
Newark Charter High School
Starting Cornell University Fall 2023

2) NASA iMaginAviation Annual Conference: A gateway to Aviation Transformation
    a. 3,265 individual registrations
    b. ULI participation in Gathertown - a Virtual Tour and Poster session with attendees
    c. Hosted iMaginAviation Watch Party at UD-CCM with 50 students attending. Organized by our local SAMPE Chapter
3) ULI co-sponsored seminar series called CCM Connects: The Future is Composites attended by 700 people.
4) Hosted Delaware Aerospace Education Foundation – Space Beam Challenge engaging 32 students (8^{th} and 9^{th} grade) in composite aerospace applications.
5) Southern University hosted 7 events involving 8 middle schools in Baton Rouge, LA. Over 1700 underrepresented minorities were involved in these activities.

With respect to Diversity, our ULI funded 14 PI/Co-PI's (14% Underrepresented Minorities (URM)) and 18 students/post-doctoral researcher. An additional 61 students (unfunded) benefited from ULI activities. Within this student group 21% were URM and 17% female. Additional details are given in the Diversity section below.

Technical Highlights

Our ULI program is organized into eight technical tasks and our Education/Workforce Training and Outreach Activities. The technical highlights and publications are provided in this section. Educational/Workforce Training and Outreach highlights are presented in the next section. Details on diversity are provided in the appendix.

The science base for microstructural design of *TuFF* composites during the alignment process and the influence of the microstructure on forming characteristics and mechanical properties of *TuFF* composites does not yet exist for this new technology. To establish the science base, we are developing a computational multi-scale framework for material selection of the constituents and micromechanics model for the prediction of anisotropic constitutive models for viscosity for forming simulations of complex geometry parts and micromechanics model for prediction of static and fatigue properties of the materials. Our overall vision is to leverage commercial software for CAD/CAM/CAE for composites and integrate the key results (material models and material databases) through custom development subroutines (UMATs) to enable design of materials, forming processes and part design using *TuFF* composites.

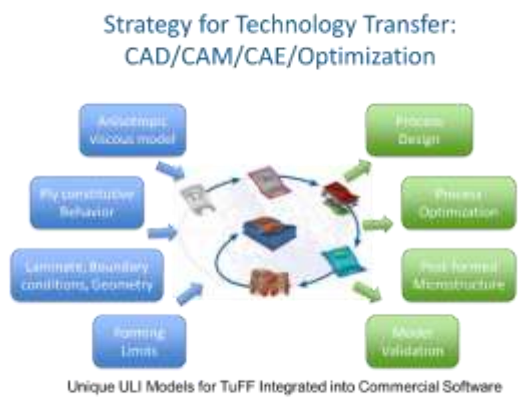

These specific technical tasks are ongoing:

1) Materials and Part Selection
2) Micromechanics of Aligned Short Fiber Composites
3) Physics of Fiber Alignment
4) Micromechanics of Anisotropic Viscosity, Constitutive Model Development and Forming Limits
5) Process Development
6) Self-Healing Composites

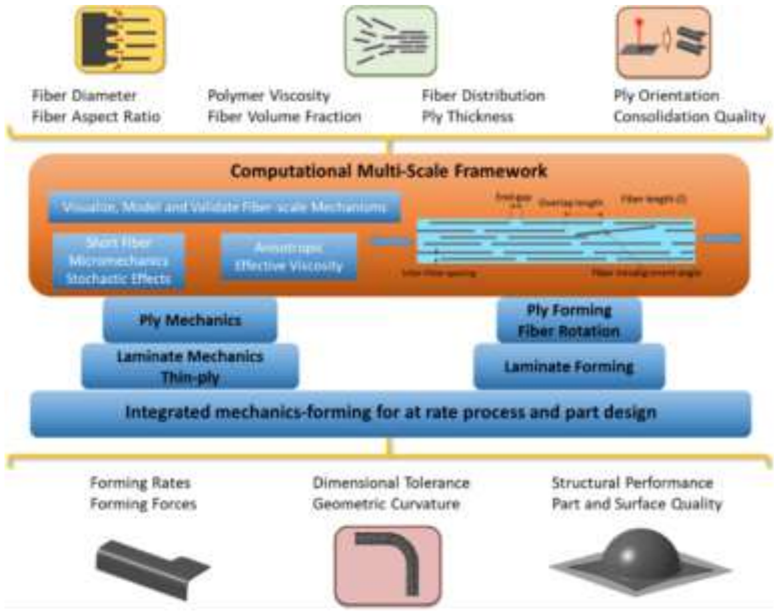

Highlight: Part Demonstrations with Industry Partners

In discussions with industry team members, various parts have been selected by Joby and Spirit Aerospace ranging from doors and instrument panels for the UAM platform to thrust reverser cascade for aircraft that are particularly difficult to manufacture with continuous fiber composites and are well suited to demonstrate the formability of *TuFF* composites. Details of our collaborative activities are included in this section. Technical meetings on TuFF forming process development, tool design and fabrication and technology transition planning was a major focus in Year 3. Parts of interest were finalized with both industry partners Spirit and Joby.

Spirit identified the Thrust Reverser Cascade (documented in last Year report) and a Window Frame as the two components for process development and TuFF demonstrations. Both parts meet the volume requirements as well as geometric complexity that has posed challenges for continuous fiber systems.

Joby identified three components: Ribs (family of geometries off a base triangular shape), Door frame, and a B-Pillar. All three components are based off the current aircraft that uses labor-intensive, complex ply pattern and layup/debulking procedures to achieve the geometric complexity needed.

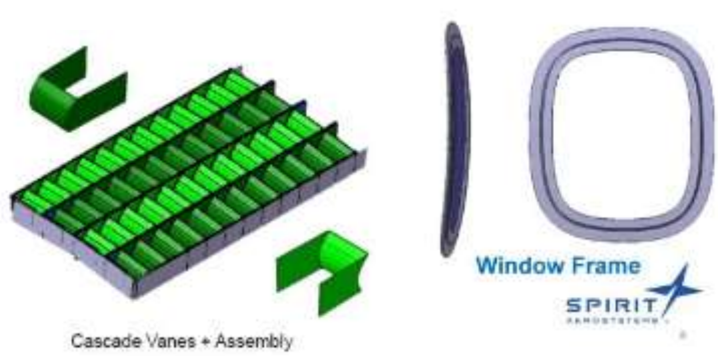

Final parts for TuFF forming demonstrations from Spirit (above) and Joby (below).

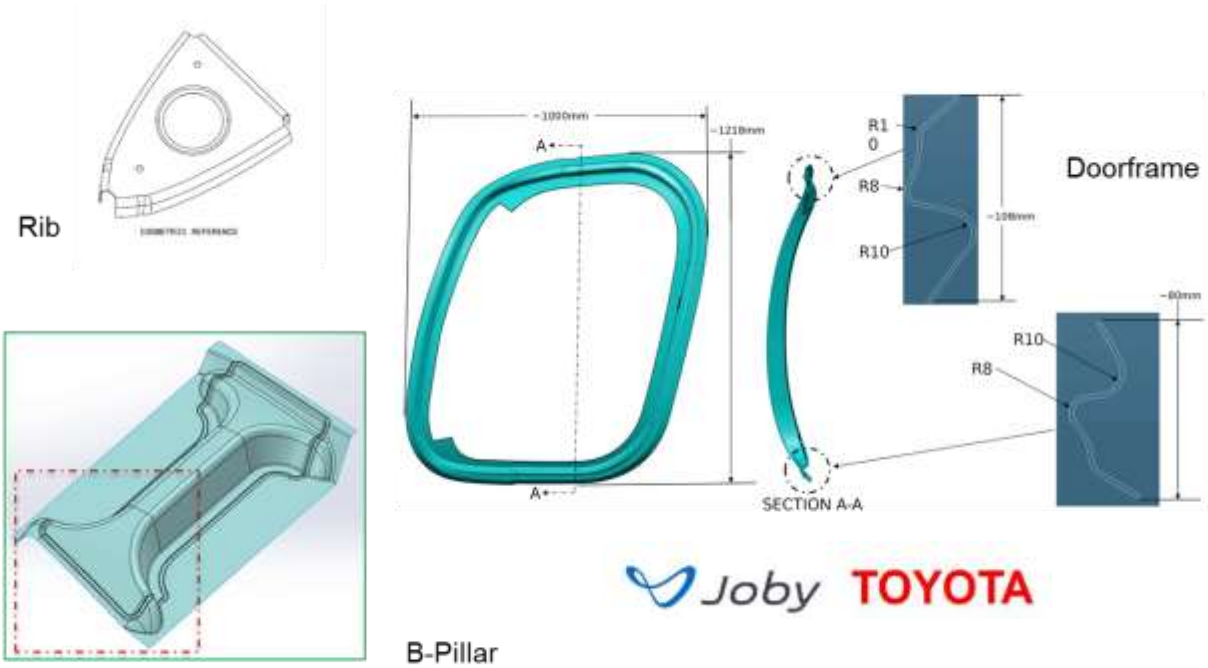

<u>Spirit Collaborative Activity and Transition Plan</u>

The cascade is an assembly of a number of vanes, of which there are two types as shown in the figure below. There are 1200 vanes per twin-engine aircraft with 600 of each type. A nominal production rate of 100 aircraft/year leads to a volume of 120,000 parts per year production. Forming assessments are initially focusing on the Forward Loading Vane (left image in Figure), to be followed by the Aft Loading Vane.

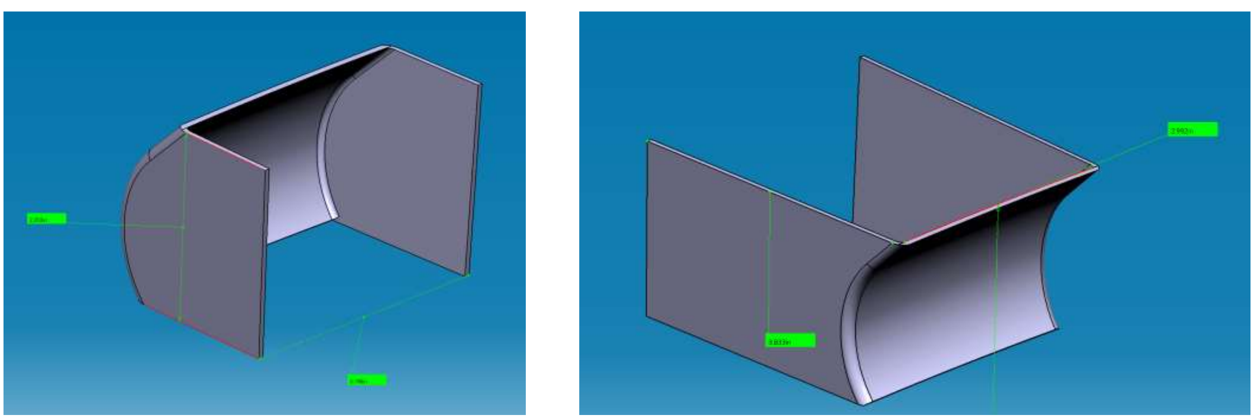

Forward and Aft Loading Vanes from the reverser cascade assembly.
Part sizes are approximately 4" (height) x 3" (wide) x 2.5" (deep).

Baseline Continuous Fiber process vs TuFF process

Cascade assemblies are currently manufactured with a time-consuming hand layup process for each vane over rubber mandrels (both aft and forward), which are then combined with strongbacks that are also laid-up on the cascade tool. The entire cascade is co-cured, followed by demolding, trim and inspection. The initial hand layup process is iterative and time-consuming, and our focus is on addressing this step through a high-volume stamp forming process, as shown below. Stamp forming individual vanes is followed by assembly and weld step (welding development by Spirit) for the final cascade.

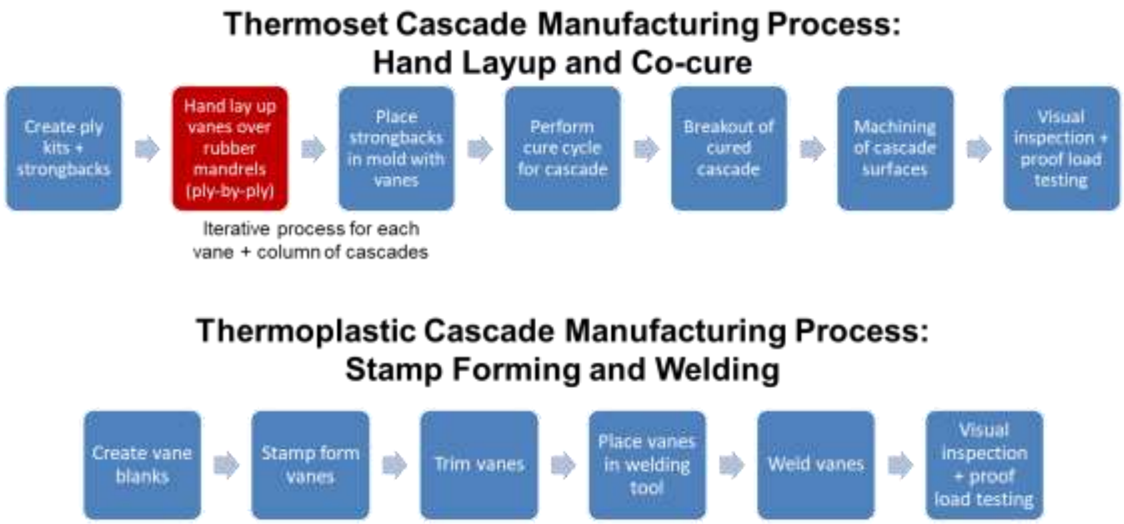

Comparison of baseline continuous fiber cascade manufacturing process (hand layup and co-cure) with the proposed high-volume stamp forming process.

Vane Forming Strategy

Forming strategy development in Year 3 focused on several aspects: forming blank design, forming strategy for TuFF and strain limits, tool design and preliminary forming experiments to assess TuFF formability for this geometry.

TuFF blank design for Vanes

After discussions with Spirit, the critical requirement for the part was identified as the effective axial modulus to address air flow and acoustic requirements during operation. The design requirement was established as > 20 Msi along the "U" axis of the vane, and a laminate design for the blank was finalized as follows:

- Fiber: 3mm unsized IM7, 120gsm FAW per ply
- Resin: LM-PAEK (Filmed and supplied by Victrex)
- Nominal 55% fiber volume fraction
- [45/-45/0_5/-45/45] ~ 45 mil thick part
- At 55% FVF effective axial modulus of 20.5 Msi with above layup
- Corner radius of vane: max 0.125" and preference is 1/16$^{th.}$
- Thickness Tolerance: +/- 5% of nominal

- Geometry: 10” x 14” (0 direction along the 10” direction) for two vanes per blank

Forming process development and strain limits

Initial forming process design focused on Forward Loading Vane, with results to be applied to the Aft Vane. Using geometry-based strain calculations, forming processes were evaluated to keep forming strains below 40%. Based on the Vane geometry (Figure 4), a combination process that includes deep draw (material translation to form the U shape) followed by forming the bottom curvature was identified as the initial approach based on the geometry and strain limits. Blank configuration and orientation were also established, with an angled orientation of the blank to reduce strains within forming limits.

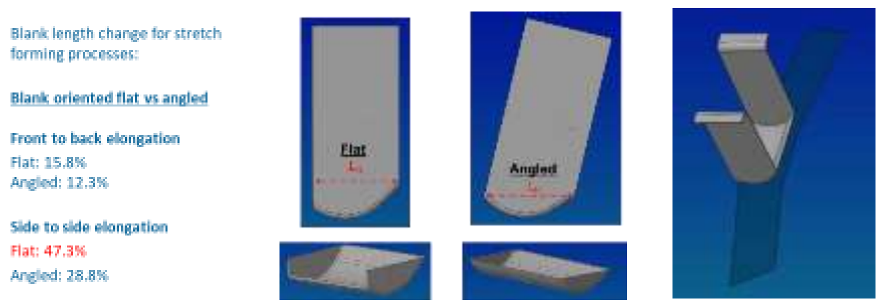

Blank configuration to meet geometry and material strain limits.

Two process methods were identified as potential candidates for Vane forming. The first is a drape forming process that relies on initial drape of the bottom geometry under tension, followed by forming the vertical walls. The second is a runner-based process, where the bottom geometry is initially formed with matched metal tool set (bottom curvature without fold), followed by tensioned forming the vertical walls of the Vane. Both process methods are shown below.

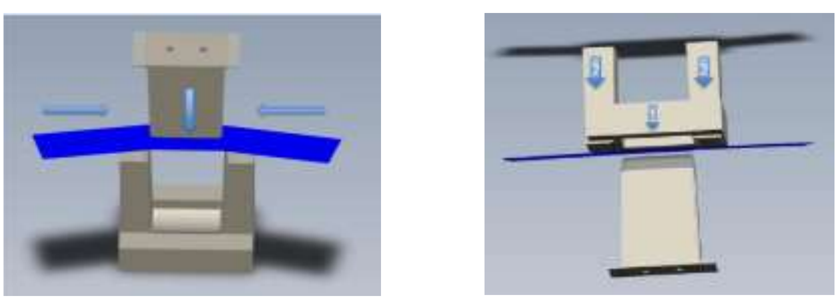

Forming strategies for Vane geometry. Matched tool set on left works with tensioned blank to address draping at the bottom curve, two-piece tool set on right is a sequential process with matched forming of the curve, followed by tensioned forming of the walls.

Preliminary Forming Experiments with Representative Geometry

Initial explorations of the geometric complexity during forming were conducted with the tool set described in Year 2 report. Isothermal forming experiments were performed with bladder and matched metal configurations with varying edge constraints. A collage of various results is shown in Figure 6 with all trials performed at 380 C, at slow forming speeds and cooling under pressure.

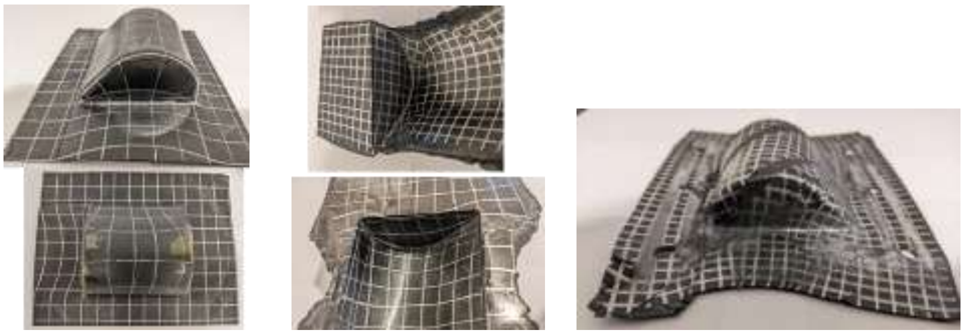

Preliminary forming experiments under isothermal conditions to evaluate blank boundary effects on formed geometry for the bottom section of Forward Vane. Left is for fully clamped, middle is for no clamping and right is for multi-axial blank in clamped conditions.

Preliminary experiments showed that:

- Pure stretch forming (fully constrained blank) results in excessive thinning even though it fully formed. While the part did not fail during forming, the significant reduction in thickness is not acceptable due to effect on performance.
- Matched metal with no blank constraints allowed a unidirectional blank to draw in fully with material folding at front and back edges. A multi-axial blank reduced wrinkles but showed the need for tensioning to eliminate wrinkles.
- Fixed edges on a multi-axial (actual blank layup) showed potential for transverse splitting of outer 45-degree ply which needs to be accounted for in blank boundary conditions.

Vane Forming Tool Design

Based on results from preliminary experiments, Spirit led the tooling design for prototype full-scale Vane forming at their facility. Team discussions between Spirit and CCM led to a tool design and process configuration which was then briefed to the NASA team on May 22, 2023. Features of the toolset and are shown below.

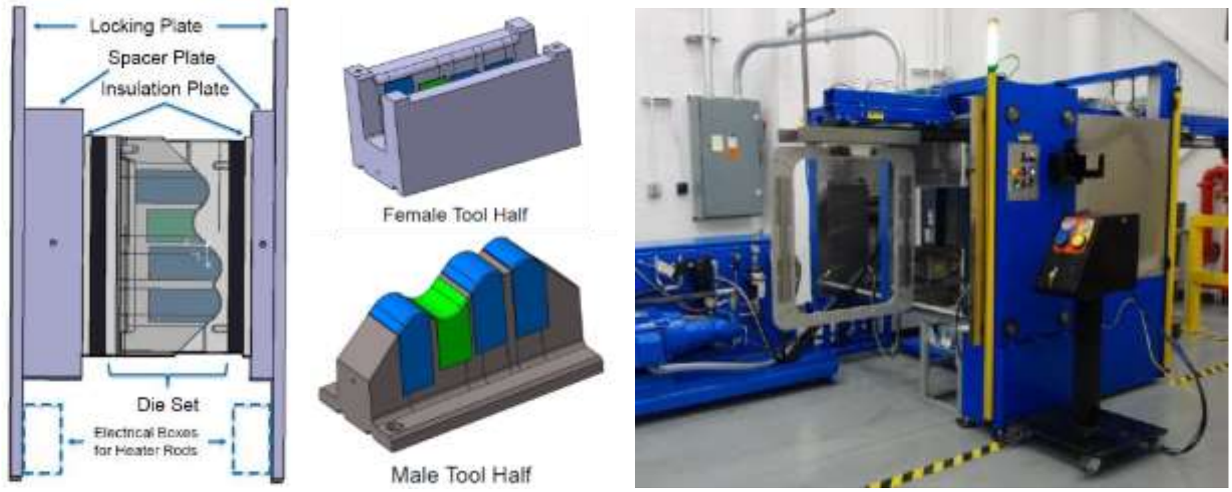

Tool configuration for Vane forming demonstrations at Spirit (left, middle) and Thermoplastic Composite Forming Cell at Spirit.

The initial forming process methodology is given below. Toolset is currently on order with trials scheduled in Fall 2023.

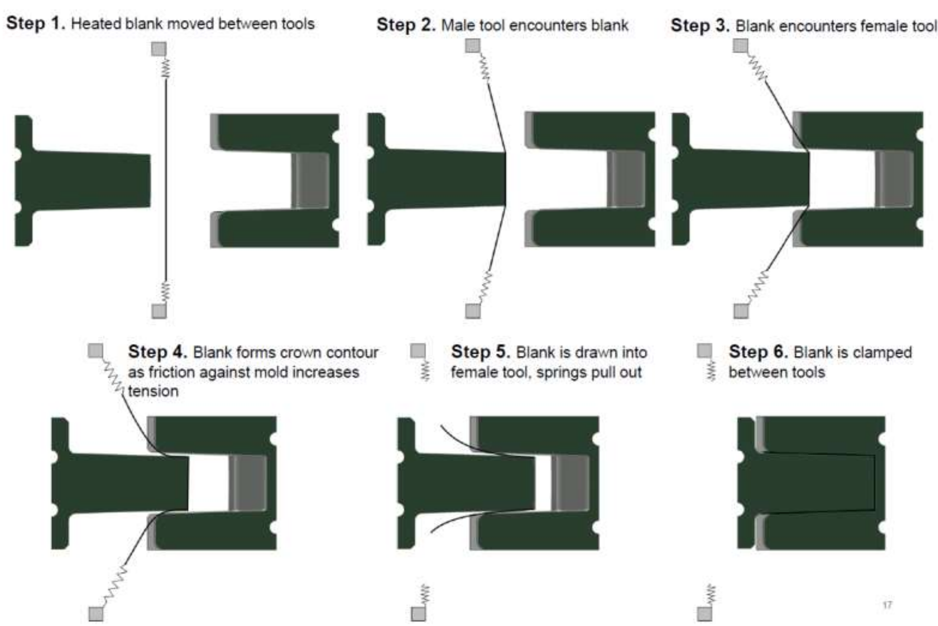

Proposed initial forming methodology for Vanes. Process will be optimized based on formed Vane quality and initial trials.

CCM/Spirit Collaborations and Activities

During Year 3, collaborative activity was centered around Vane forming process development and tool design. TuFF blanks (IM7/LM-PAEK) are being periodically shipped to Spirit for initial process trials on a standard angle-bracket tool (ILT geometry), to provide initial experience in handling and forming with TuFF blanks and material format. A schedule for Year 3 and Year 4 activity is shown with forming work for the Vane to start in Fall 2023. We expect a number of site visits to Spirit during Vane forming trials, during the course of Year 4.

	2022	2023				2024		
	Q4	Q1	Q2	Q3	Q4	Q1	Q2	Q3
Forming model experiments **(at CCM)**								
Drape Form process								
Blank boundary conditions								
Process development with TuFF **(at Spirit)**								
Downselect Vane forming process **(CCM/Spirit)**								
Tool design/fabrication **(Spirit/CCM)**								
Vane manufacturing **(at Spirit)**								
Demonstrator cascade assembly **(at Spirit)**								
Window frame								

Proposed schedule of activity for Spirit Transition Plan. Vane forming trials are expected to start in Fall 23, along with preliminary work on the Window frame part.

<u>Joby Collaborative Activity and Transition Plan</u>

Year 3 activity with Joby focused on finalizing part selection, part forming demonstrations and transition planning. Part selection was expanded to focus on three (3) relevant parts for their Urban Air Mobility platform – Triangular Rib (geometry family), Door Frame (identified in Year 2) and the curved section of the B-Pillar. These represent the final part of interest in this effort with TuFF/thermoset systems to demonstrate manufacturability and gains in cycle time and cost. A common thread in all parts is complex geometry with both local feature changes as well as global double curvatures that is currently being fabricated by hand layup. Current production process involves complex ply patterns to account for geometry, full part debulking every two plies during the layup process, followed by autoclave cure. Program goals are to evaluate manufacturability using TuFFs' stretch capability and establish improvements in simplifying ply patterns, reducing debulking frequency and improving manufacturing throughput/cost.

Part Selection and Goals

As mentioned previously, three parts from the current Joby aircraft were chosen for forming demonstrations with TuFF (see figure below). The Triangular Rib represents a family of geometries of similar shape (both triangular and rectangular) with standard geometric features – curved sides (with joggles) as well as surface features (become cutouts for systems integration). Forming the curved sides with joggle is the main challenge with the current process involving continuous fabric prepreg with hand layup and debulking sequences.

The Door frame features large curvatures in two dimensions (along length and width) as well as local features for sealing interfaces similar to automotive doors. This part represents two levels of geometric complexity with local (sealing interfaces) and global features. The B-Pillar is a more recent addition with interest primarily in the curved sections at the bottom and top and as similar curvatures as the door both in both directions. Of particular note, is that all parts for Joby were thermoset demonstrations due to the current aircraft use of thermosets with planned switch to thermoplastics in the future.

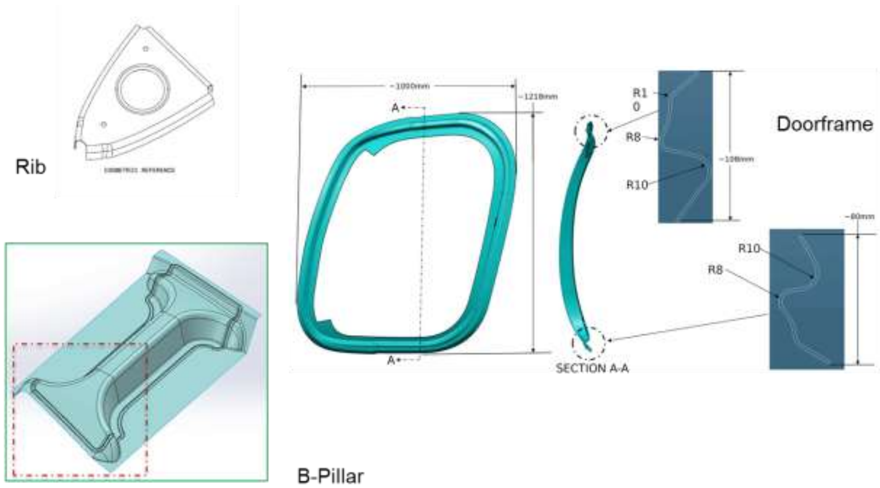

Final part selection for Joby representing multiple levels of geometric complexity and combined features. Ribs represent the starting geometry, followed by the Door Frame and the Pillar.

Rib Forming Demonstrations

Early focus in Year 3 was on Rib forming demonstrations both at CCM and at Joby. The general approach was to fabricate a full thickness blank, followed by forming the blank into the Rib geometry. A triangular Rib tool was shipped to CCM by Joby for forming experiments as shown in the figure below1. The tool is a two-piece design with a nominal rib depth of 1" and was selected as a representative geometry. Note that a full stretch forming process would require greater than 100% stretch to form the geometry, hence a combination of draw and stretch was evaluated for this part.

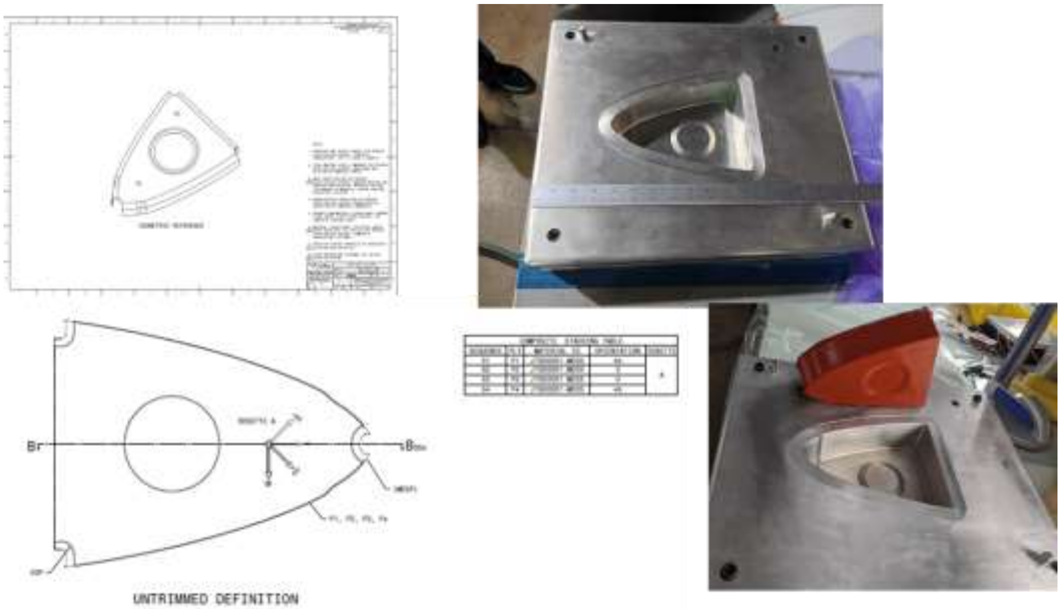

Triangular Rib part detail and Tool. The Rib is a 4-ply design which is duplicated in TuFF prepreg blanks. A silicone male plug (in red) was cast to provide a male tool during forming and cure.

Process trials were conducted with TuFF/thermoset prepreg, based on 3mm IM7 fibers and Axiom 5201 epoxy resin as these trials can be performed at room temperature to demonstrate formability. A number of initial trials were conducted ranging from drape forming on the male plug and direct forming into female plug, under vacuum pressure. The figure below shows a vacuum drape forming example.

Vacuum drape forming of Triangular Rib with flat debulked TuFF prepreg blank. TuFF stretch-forms the dimple, however wrinkles (right side photo) are seen on the curved flanges.

Wrinkles during forming are the result of compression strain induced due to the geometry and can be overcome with tensioning the blank appropriately. A tensioning frame with spring/tab boundary conditions was designed and implemented as shown below. The blank is fabricated with hand layup and debulk in its flat configuration, compared to in-tool debulking which is significantly more complicated. The flag prepreg blank is tensioned in the frame and the male plug used to form the shape (vertical downward pressure on male plug so the blank is formed into the cavity), followed removal of the male plug, bag, and cure. The cured part shows good geometric conformity in the dimple (stretch-formed) as well as around the curved flanges of the Rib, including the joggled edge.

Tensioned forming of Rib with TuFF prepreg blank. Tensioning frame/springs with prepreg schematic (left), Cured Rib showing surface dimple and joggled curved flange.

Following the forming demonstration for the Rib, a Thermoset Forming Cell has been designed and implemented at CCM, with the Rib toolset so that calibrated experiments can be performed to understand and establish forming process guidelines for TuFF thermoset blanks. The Cell is designed to conduct mechanism-based experiments to understand influence of blank boundary conditions (tensioning parameters, tab design), forming rate (press closure rates), temperature and R/t for thicker prepreg blanks on formed part quality with the Rib as the candidate geometry. The goal is to establish a process guidebook that provides Joby with all the necessary information for forming TuFF parts at their facility.

TuFF Thermoset Forming Cell established at CCM. The Cell enables various blank boundary conditions, forming temperatures and process variants to establish TuFF Forming guidelines.

UD-CCM/Joby Collaborations and Activities

Year 3 saw significant collaborative activities with Joby engineers including multiple visits to CCM (Year 2 Annual Review in Oct 2022, Nov 2022 site visit for forming trials, Mar 2023 site visit for forming trials and transition plan discussions), as well as UD-CCM visits to Joby (Oct 2022 after CAMX, Jan 2023 for forming trials at Joby). In addition, Joby's Fiber Placement visited UD-CCM for a tape steering demonstration of TuFF and its capabilities.

Joby is also establishing a new R&D center in 2023 at Santa Cruz with infrastructure for forming research and development including a large-scale press (nominal 2' x 6') for both scale-model and full-scale prototype development. Transition of results from joint UD-CCM/Joby work is expected to occur at this facility in Year 4.

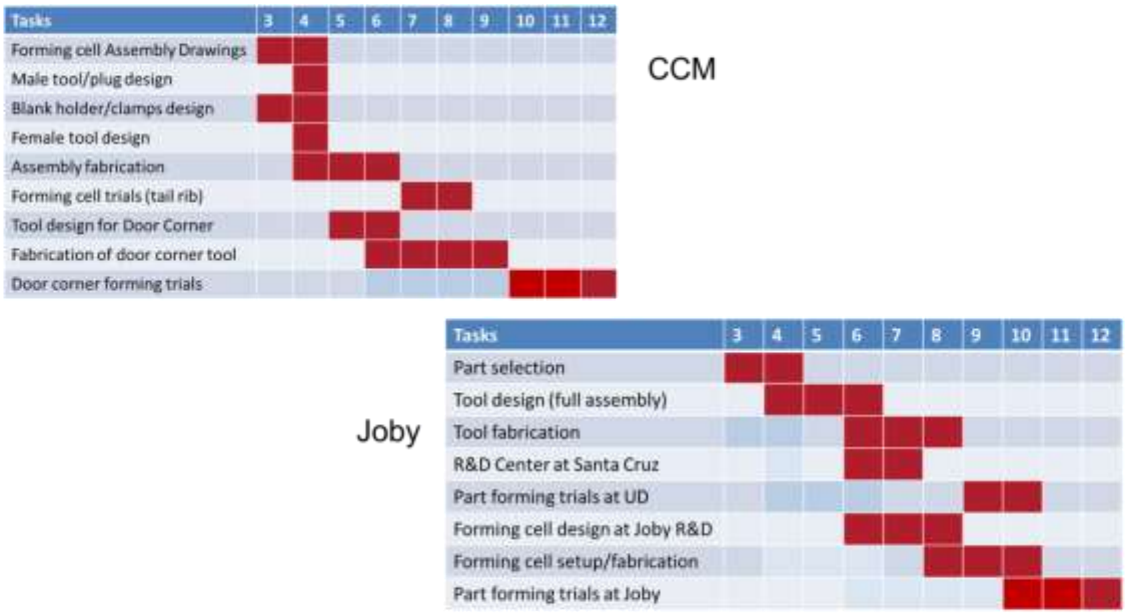

Proposed schedule of activity for Joby Transition Plan in 2023 (columns are months). CCM will focus on forming process development and prototype demonstrations, Joby will establish forming infrastructure and initiate forming trials.

In Year 4, full-scale door frame demonstration is proposed with the tool system already shipped to CCM from Joby. This will include forming demonstrations of critical sections followed by a full-scale door article demonstrator. Joby will conduct a metal part replacement study with an assessment of existing Aluminum parts on Joby aircraft and potential for TuFF composite replacement. A key aspect of Year 4 is a part repeatability assessment and one of the ribs will be selected for evaluation. Repeat manufacturing up to ten (10) parts will be performed at Joby's facility followed by a cost assessment – TuFF approach vs continuous fiber. An at rate production demonstration is planned to demonstrate forming at rate and fast cycle times, as well as a thermoplastic forming demonstration and cycle time.

Highlights: Constitutive Behavior and Micromechanics of Anisotropic Viscosity

A set of constitutive laws for the material behavior during forming are be constructed for the purpose of developing process models and a forming simulation capability. The fiber direction is the primary load carrying material orientation in forming, so a set of experimental methods were developed measure local material deformation during longitudinal extension. The approach is to develop macroscale constitutive behavior with respect to temperature and strain rate, while simultaneously investigating the micromechanics problem. In the previous year, it was demonstrated that the micromechanics will underpredict both the extensional viscosity and the shear magnification. Here, we are focusing on investigating the viscoelastic behavior of the material—to understand the shear magnification—while developing a revised micromechanics model to better predict the shear magnification.

Like the thermoplastic polymer matrix, the composite material can be described as a viscoelastic fluid. When loading at constant strain rate, the material will deform elastically and then transition to viscous after passing the relaxation time—as predicted by the Maxwell fluid model. After reaching the peak stress, the viscous deformation is strain softening (due to microstructure effects). When the displacement is held constant, the material stress relaxes to zero.

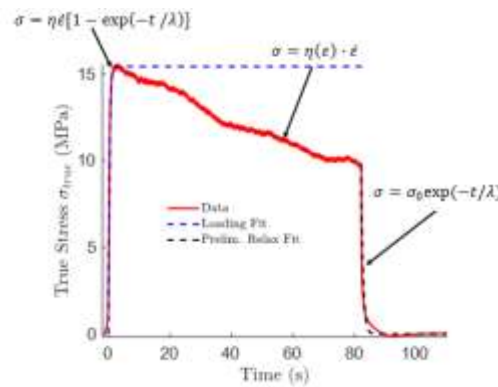

<u>Viscoelastic Behavior</u>

The maxwell model is fit to the initial loading portion of the material tested at constant strain rate. This allows the relaxation time to be measured. The elastic modulus is computed as the ratio $E = \eta/\lambda$. TuFF/PEI samples were tested at tempeartures 250-350C, at strain rates 1e-4 – 1e-1 s^{-1}. Previously it was shown that viscosity and strain rate can be shift to a common reference temperature using the polymer TTS shift factor a_T. The viscosity was shown to follow a power law behavior with strain rate. The single model Maxwell model provides a good fit to the material behavior for loading under constant strain rate. The measured relaxation times also follow a power law behavior with strain rate, which suggests that an underlying micromechanics mechanism is influencing the results (e.g. onset of strain softening). The correlation of loading relaxation time and viscosity has a power law relationship. The strong correlation of this relationship means that the loading behavior of the material can be directly predicted. The relaxation time determined by this loading regime is smaller than the relaxation time observed in stress relaxation (shown above).

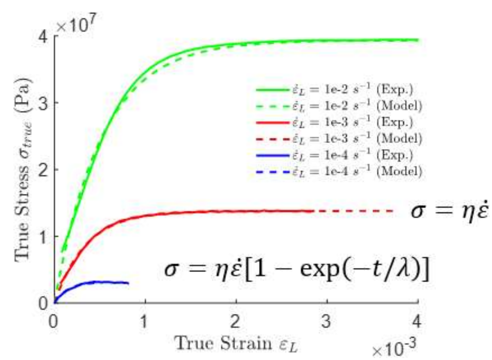

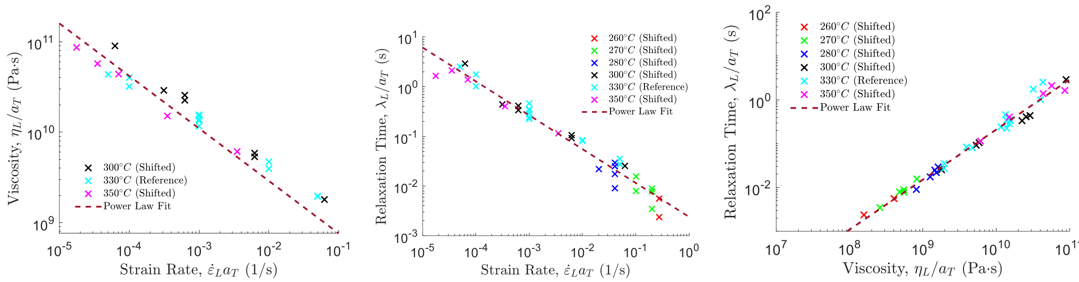

Strain Softening

To investigate the strain softening behavior with respect to process conditions, single ply TuFF/PEI samples were stretched at a constant strain rate of 0.001 s^{-1}, and temperatures between 280-350C. Samples tested at 310 and 320C had the highest extensibility, with no indication of strain localization. The stress strain curves were normalized by the peak stress in order to compare the strain softening slope.

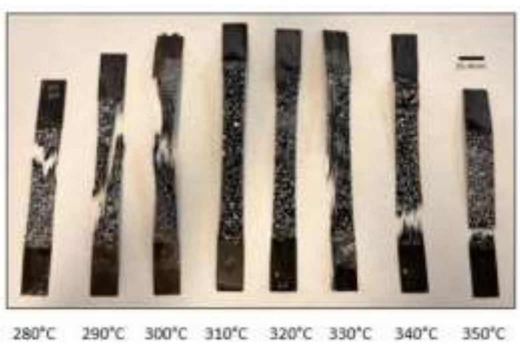

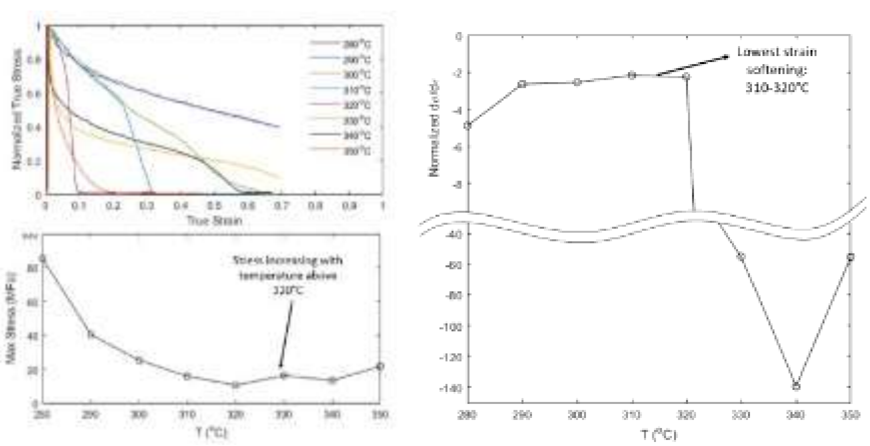

The normalized strain softening slope at the onset of viscous extension was between -5 and -2 for temperatures below 320C and abruptly decreases for temperatures 330-350C. Several other complex strain softening transitions are observed in the data as strain increases in different temperature ranges.

Micromechanics for Prediction of Extensional Viscosity

A set of modifications were developed for the unit cell micromechanics model to correct for (i) high viscosity, (ii) high shear magnification, (iii) material porosity, and (iv) changes in fiber overlaps with strain.

$$\eta_L = \left[\frac{-\beta V_f}{2\ln\sqrt{\zeta\beta V_f}}\right]\left(\frac{L}{d}\right)^2 \left(\hat{L}_s\right)^2 \eta_P\left(1-\phi_r\right)$$

The derived model groups porosity into the resin phase $\left(1-\phi_r\right)$ to affect the polymer viscosity and includes a dimensionless shear length which is a function of strain. If all fibers translate uniformly, fiber overlaps will decrease linearly with the applied longitudinal stretch, $\hat{L}_s = L_s/L_{s,0} = \left(2\exp\varepsilon_L - 1\right)$.

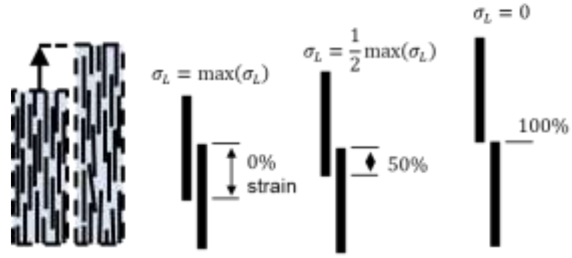

Another major contribution of the model is a modification parameter to increase the shear magnification. The existing micromechanics model compute the fiber spacing based on the fiber diameter and fiber volume fraction, thus assuming that fibers are uniformly spaced. In reality, fiber spacing will vary radially and along the fiber length according to a distribution. In areas where spacing approaches zero, strain rate approaches infinity. To correct for this statistical distribution, the cell model is allowed to have a characteristic outer radius $R_{o,c} = \frac{1}{\sqrt{\zeta}}\langle R_o\rangle$ which is less than the volume averaged radius $\langle R_o\rangle$, by a distribution parameter referred to as ζ. The parameter is bounded, $1 \leq \zeta < \frac{1}{\beta V_f}$. ζ equals 1 when all fibers are uniformly spaced (minimum shear magnification) or can increase until fibers are touching ($\zeta = \frac{1}{\beta V_f}$ when $R_{o,c} = R_i$ and $\eta_L = \infty$).

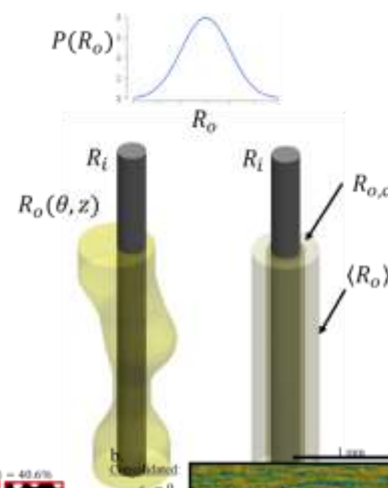

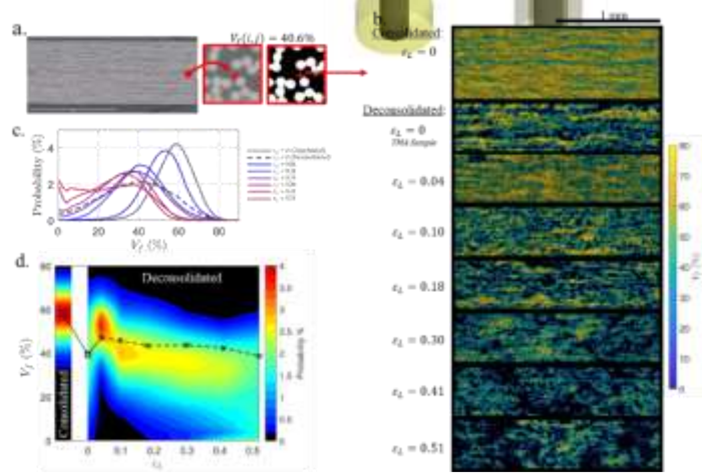

The experimental data shows that the local fiber volume fraction (and fiber spacing) will vary and change as the material stretches. Material porosity will also be present during deformation and slightly increase with strain ($\phi(\varepsilon_L) \approx 0.26\varepsilon_L + 0.18$). Likewise, fiber volume fraction decreases with porosity ($V_f = V_{f0}(1-\phi)$).

The spacing distribution parameter is used to fit to the micromechanics model to the material data at the point of peak stress (before strain softening begins). In this deconsolidated state, the fiber volume fraction is 47%. The volume averaged fiber spacing is approximately 2 μm, however, based on $\zeta_0 = 1.77$, the characteristic fiber spacing is 0.2 μm. The increase in porosity has a contribution to strain softening. The change in fiber spacing cannot be determined as deformation progresses. If ζ remains constant at 1.77, the model will under predict the material response.

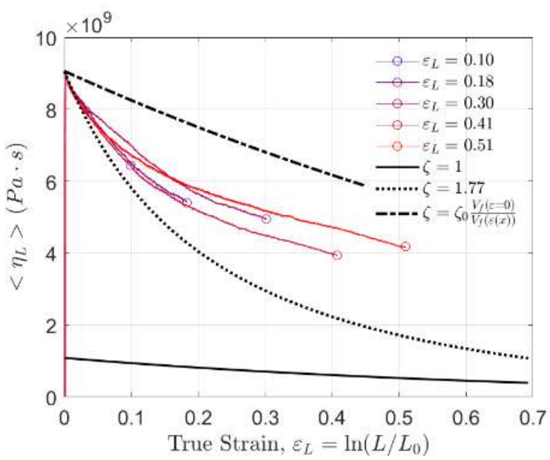

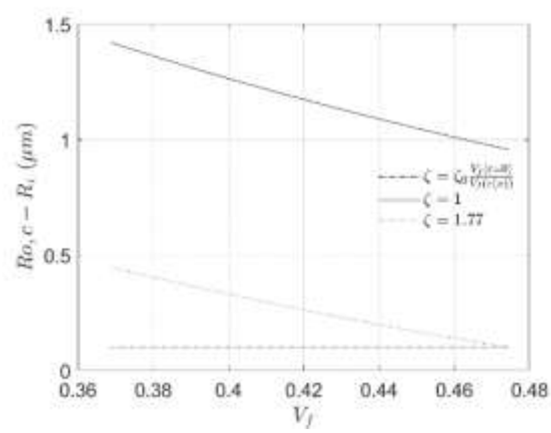

If fiber spacing remains constant, $R_{o,c} = 0.2\ \mu m$ (corresponding to $\zeta = \zeta_0 \left(V_f(\varepsilon_L = 0) / V_f(\varepsilon_L(x)) \right)$), then the model over predicts the material response. The shear length term ($\hat{L}_s$) for estimating the loss of fiber overlaps can be used as an additional strain softening mechanism. This term is evaluated for the case when characteristic fiber spacing remains constant at $R_{o,c} = 0.2\ \mu m$. By normalizing the data and comparing to the model $\hat{L}_s = L_s / L_{s,0} = (2 \exp \varepsilon_L - 1)$, it can be seen that the dimensionless shear length exceeds the model for strains above 0.15.

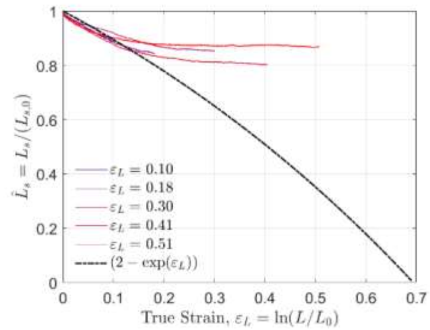

The conclusions from this micromechanics model are that fiber spacing distribution will contribute to an order of magnitude increase in the measured extensional viscosity, the fiber spacing will not relax during deformation, and that fiber overlaps in the microstructure will recover during extension. This recovery of fiber overlaps is the primary mechanism for ply thinning during stretch forming (reported in the previous year).

Suumer Undergraduate Research Profiles

Charles Whealton is an Honors Junior Mechanical Engineer at the University of Delaware. He is the Secretary of ASME at UD and works as a TA. He plans to pursue a doctoral degree in Mechanical Engineering and work in higher education.

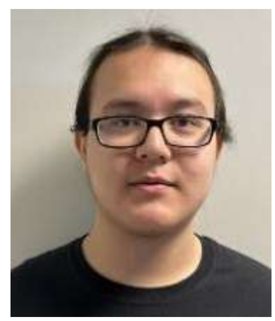

"The NASA-ULI has helped me get first-hand experience.
with multi-faceted research and gather an understanding of
what I want to do in my career."

Project: *Characterization of Viscoelastic Material Response of Highly Aligned Discontinuous Fiber Composites*

Charlie is working to understand the viscoelastic material behavior by experimentally characterizing TuFF samples with new test protocols and implementing viscoelastic models. He is planning to extend his results (mentioned above) to measure the stress relaxation behavior of TuFF, implement a multimode Maxwell model, and understand how the relaxation behavior can bring new insights to the material microstructure.

Owen Ferrone is an Honors Junior Mechanical Engineering student at the University of Delaware who is extremely passionate about all thing's math and science. He participates in programs as a member of both the UD Honors College and the UD Blue Hen Leadership Program.

Project: *Stretch Forming of IM7 Thermoplastic TuFF Composites: Effects of Environmental Conditions on Forming Optimization*

Owen is investigating the effect of process conditions on the formed material quality. His work (above) has shown that forming of thermoplastic matrix TuFF is highly sensitive to temperature. He plans to continue this work to investigate the effect of strain rate on forming quality. Once understanding the effect of process conditions on formed material quality, he will conduct tests to determine the mechanical properties of TuFF after stretch forming.

Controlling Deconsolidation

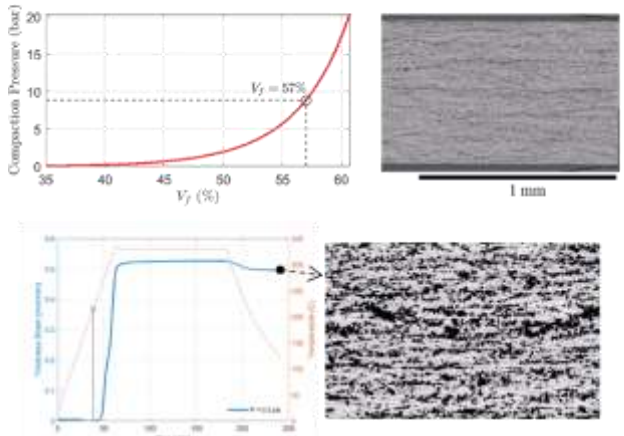

As reported in our Year 2 Annual Report, the pressure required to consolidate composites is a function of the microstructure. To achieve aerospace performance fiber volume fraction of 57% requires a high degree of fiber alignment and blank consolidation pressure of 300 psi. During forming, the blanks are reheated to process temperature without pressure (our robotic forming cell uses an IR oven). Both continuous fiber and our aligned short fiber thermoplastic TuFF composites will deconsolidate in this case (up to 50% increase in thickness is measured).

Research in this area is studying the deconsolidation characteristics of TuFF, the effect deconsolidation has on forming, as well as processing to control deconsolidation during forming. Initial work looked at the dry compaction behavior of the fiber bed to understand the material compliance, as well as the deconsolidation in the prepreg level for heat cycles in a TMA. The thickness change and microscopy agreed with the dry compaction data, that TuFF will deconsolidation from 57% to 39% FVF upon heating without pressure, resulting in a 50% increase in thickness.

Full blanks were analyzed in a Keyence 3D scanner to determine thickness profiles before and after deconsolidation, as well as for samples after forming. The 3D scanner has a resolution of 10 µm, which results in an accuracy to within 20 µm when computing thickness. Consolidated blanks showed thickness variability on the order of the scanner accuracy. After deconsolidation, the blank thickness grew uniformly with the exception of select location which showed higher deconsolidation. This phenomenon is linked to misaligned fiber cluster defects which have a known frequency in the material. After forming, the thickness variability is shown to be variable. It is not yet clear how the deconsolidation effects the strain variability and thickness after forming.

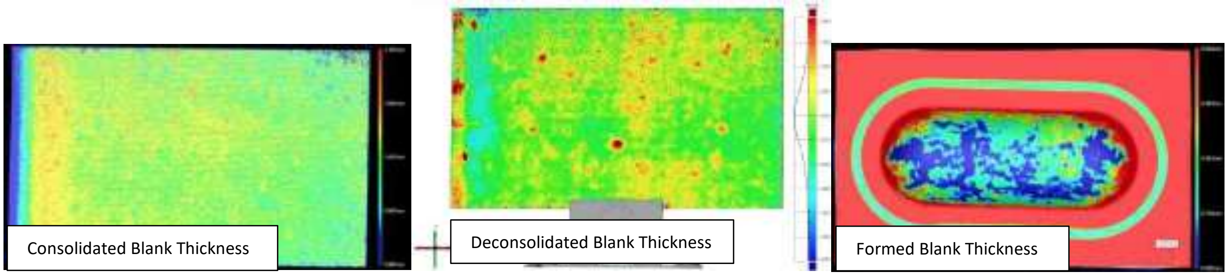

One method to control deconsolidation is to confine the blank during form. This is accomplished with a double vacuum bag. The blank is enveloped between two layers of Upilex 050RN film and the gas pressure on both sides of the blank is controlled. The blanks are placed in a tool cavity, pressurized to 0, 15, 50, 100, 200, and 300 psi from one side and the material is compacted against a flat tool surface. The temperature of the press is cycled up to 380C and down to room temperature. After deconsolidation under controlled pressure, the samples were measured to determine thickness growth and thermal diffusivity. The sharpest decrease in deconsolidated thickness is achieved for the first 15 psi of pressure, which indicates that vacuum bag confinement of the blank may have a substantial impact/improvement in formed material quality. These results also indicate that blank processing under vacuum only would provide a more stable blank during forming (with the final consolidation pressure after forming remaining 300 psi).

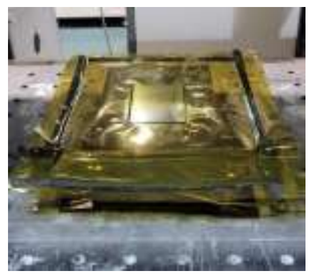

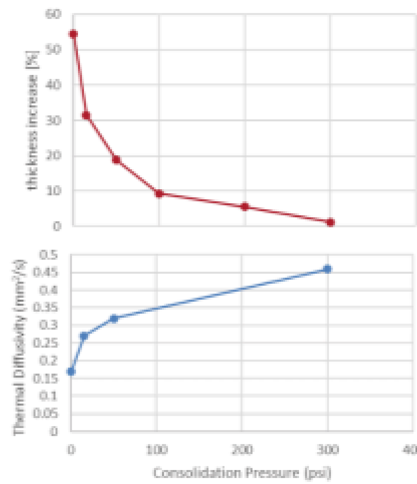

To investigate the effect of confinement pressure controlling deconsolidation on formed material quality, LM-PAEK/TuFF blanks were processed in a bladder molding cell with a constant pressure from the tool side of 0 or 15 psi gage pressure. The recommended processing temperature for LM-PAEK is 380C; however, based on the results above (strain softening) indicating that

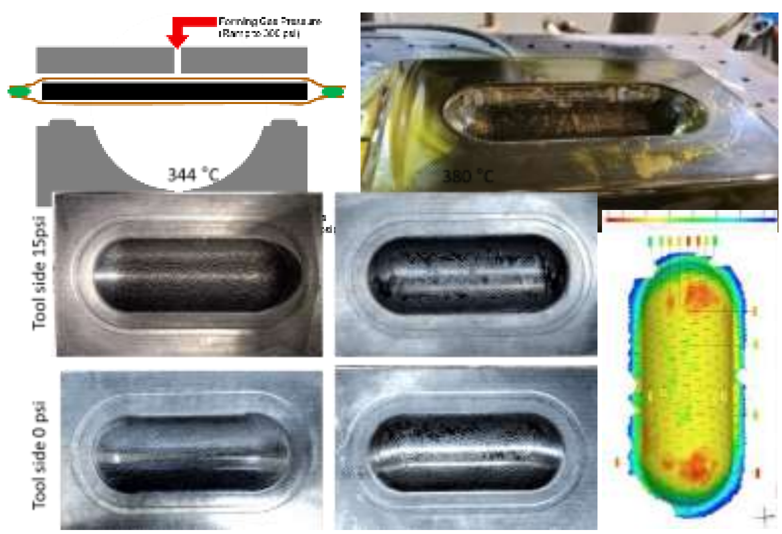

high temperature may be detrimental to forming. Samples were formed at temperatures of 344 and 380C. The results of the study show that the sample formed at 344C with a tool side pressure of 15 psi measured the highest uniformity in the strain pattern by photogrammetry.

New Thermoplastic Composite Forming Capabilities at UD-CCM

Composite material forming characterization was acquired under DURIP-ONR FY22 - N00014-22-1-2124 “Material Characterization for Highly Formable TuFF Composites”. The new system was installed in July 2023. It includes a GOM optical measurement capability to measure surface strain in-situ (with DIC) during forming, or ex-situ (with photogrammetry) in closed mold processes. The system also includes a servo-hydraulic press from Interlaken which was adapted for hot metal forming material characterization.

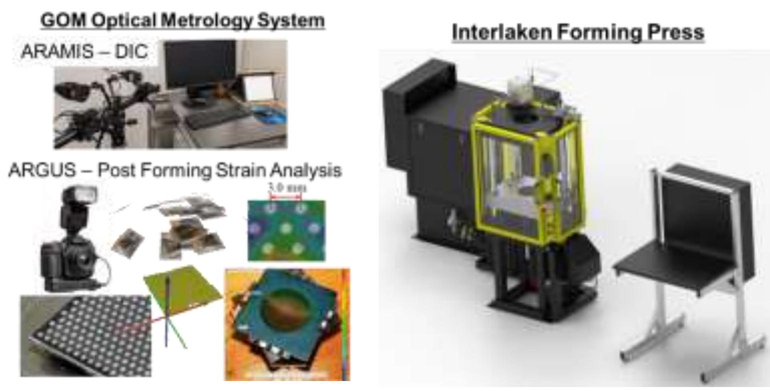

The Interlaken forming press was customized with a C-axis Sapphire sight glass, gas pre-heat system, and heated tool sets in order to conduct isothermal forming experiments with direct in-situ visualization.

The press action consists of a heated hydraulic frame, which clamps blanks with a binder ring, and central punch. The punch can close at a rate 3 in/s, which is consistent composite stamping processes used to achieve 3-minute cycle times.

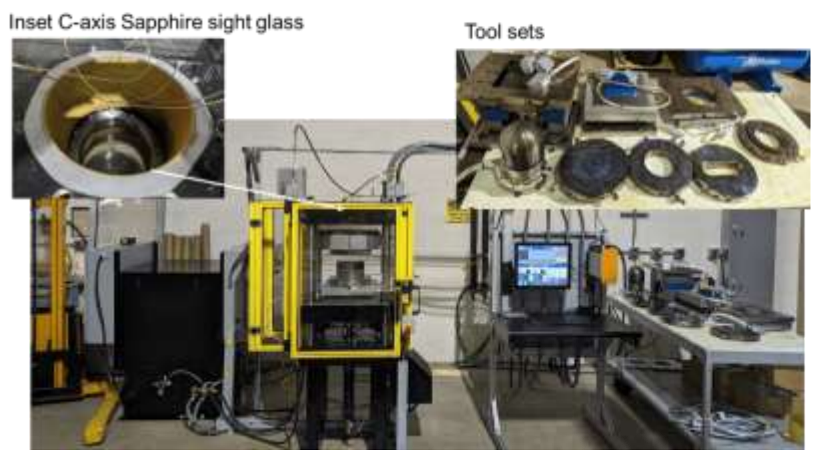

The hemispherical tool sets are designed to investigate deep drawing and tool ply interaction. The flat tool sets are design for imposing defined strain modes (plane strain or biaxial strain) which can be used to extract flat mechanical test coupons. The hot gas bulge system will be used to obtain material constitutive laws (in place of

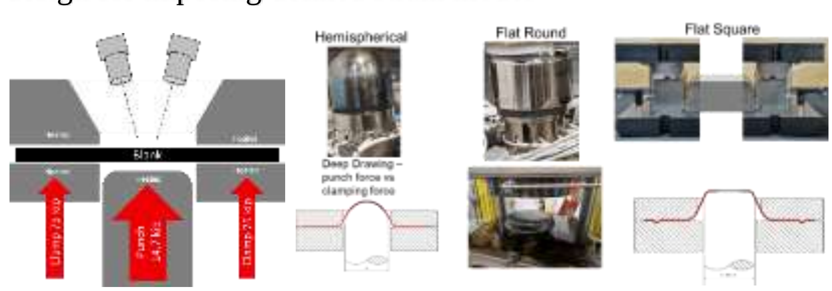

the current Instron extension testing) to determine the effect of strain mode on the constitutive behavior of the material.

To achieve aerospace level of mechanical properties with aligned short fibers, it is essential to achieve excellent fiber alignment within the preform (i.e., 95% of the fibers within the preform are aligned within +-5°). This is required to enable high fiber volume fraction (57%) during prepreg manufacturing to be achieved. Fiber breakage during the alignment process must also be minimized to retain unimodal fiber length distribution (see project on Physics of Fiber Alignment below). In addition, high levels of interfacial bonding between the unsized carbon fiber and the LM-PAEK is required. In our past work with IM7/polyetherimide an interfacial shear strength exceeding 60 MPA is required to achieve properties equivalent to continuous fiber composites. Last year, single fiber pull-out experiments with an embedded length of 50 microns provided and outstanding level of bonding between IM7 and LM-PAEK with an Interfacial Shear Strength (IFSS) of 128.7 +- 20 MPa.

Forming Software: Aniform

This task aims at identifying commercial software platform to simulate the forming process of the *TuFF* material. In Year 2 of the ULI, a collaborative project with Altair was undertaken to assess the capability of Hyperform's existing material models to model the stretchability of *TuFF*. The conclusion of this study was that Hyperform was not able to model the highly anisotropic viscoelastic behavior of TuFF and the numerical simulations were not stable. In parallel, during Year 2 and ongoing in Year 3, our team initiated discussions with the developers of Aniform using Air Force funding (Low Cot Thermoforming). Aniform has worked closely with our team in implementing TuFF constitutive behavior and providing technical support. In Year 3, our ULI has leveraged the findings of the Air Force Program. Our plans are to use Aniform for simulating the Spirit and Joby demonstration parts mentioned above. The Aniform results generated on our ULI bead molds are promising.

The aim of this task is to obtain numerical tools to map the original configuration of Tuff material sheets to the final one *after* part forming. This should include fiber orientation and ply thinning or thickening. In addition, Aniform added temperature solution and the company was willing to work with us to develop user material for linearized Tuff constitutive relation (Beaussart fluid) as applied to thermosetting resins and Tuff prepregs. As a result, software system capable of "virtually forming" Tuff parts. The Aniform, as it is now (version 5), provides:

- Modeling for a variety of composite forming processes.
- Reasonable selection of ply-to-tool and ply-to-ply interaction models
- Constitutive equation for Tuff Material sheets
- Tracking of important parameters (thickness, fiber orientation) throughout the forming process

Aniform forming capabilities are highlighted below. Generally, Aniform is suitable for forming any Tuff material – thermoplastic or thermoset. The application to ULI TuFF materials and parts is planned for Year 4 but it requires establishing of different model parameters, both for the material (being developed) and material/tool interactions. The new forming capabilities mentioned above (ONR DURIP) is highly instrumented for real time temperature and deformation measurements will be essential for determining material/model parameter for Aniform simulations.

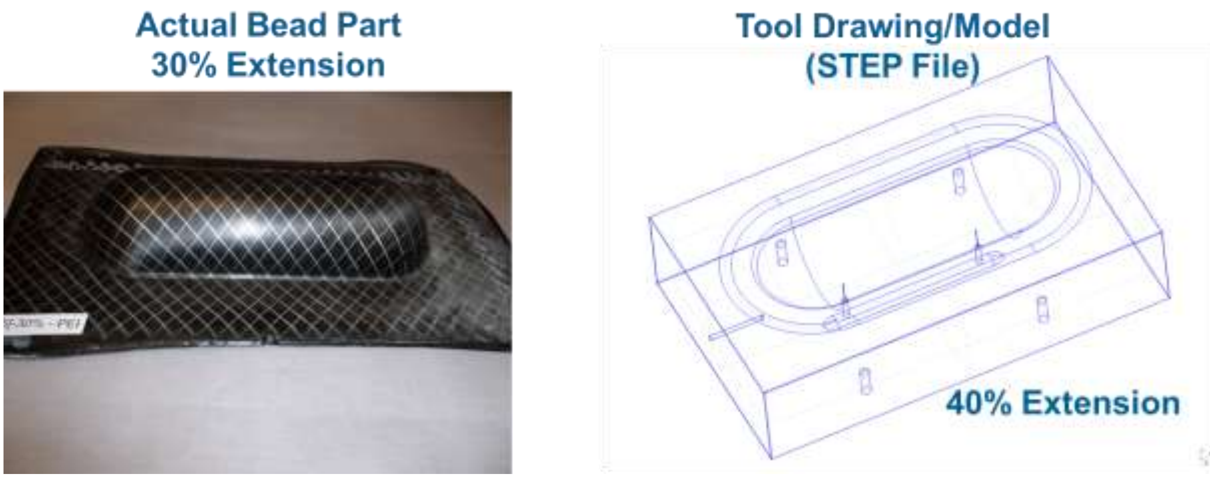

Formed Thermoplastic bead and the mold geometry.

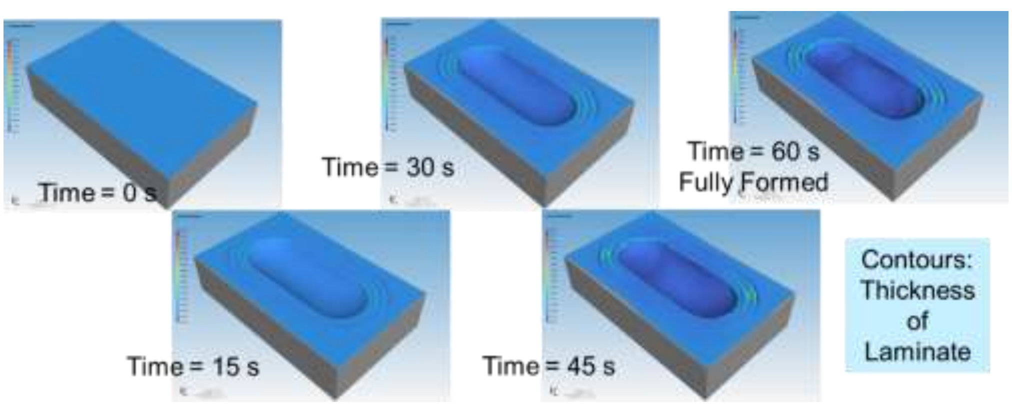

Aniform model for +-45 degree bead during virtual forming

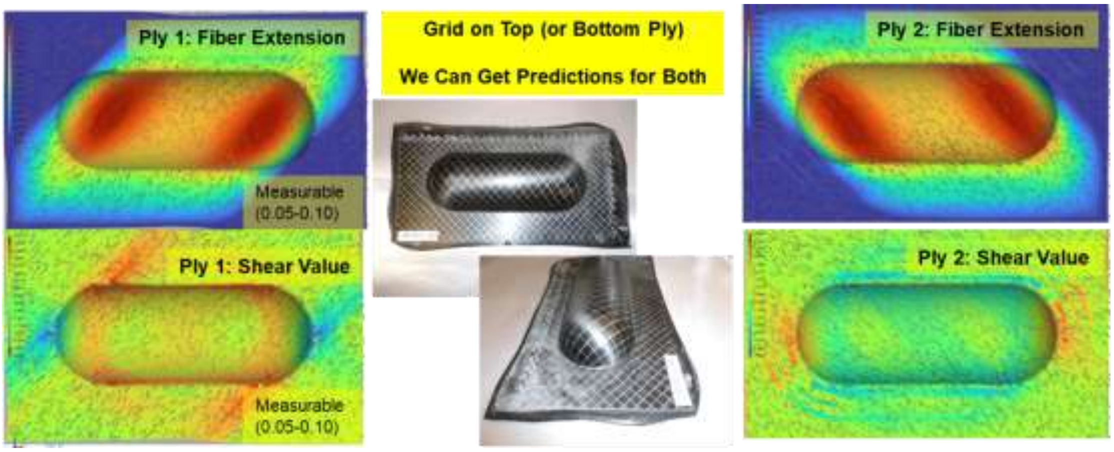

Aniform model for +-45 degree bead during: Predicted deformation for each ply.

Highlights: Steering of TuFF Carbon Fiber Thermoplastic Tape with Automated Fiber Placement

Topology optimization of continuous fiber-reinforced polymer composites can be constrained by material and processing limitations. For example, Automated Fiber Placement (AFP) can locally steer the fiber orientation within each composite layer enabling the stiffness and strength of laminated structures to be optimized to reduce stress concentrations suppress buckling modes or passively control deformation for increased weight savings. Advanced tow placement equipment uses a robotic head to steer the tape along programmed paths. The primary manufacturing constraint is the Minimum Steering Radius (MSR) achievable without defects. Our ULI has two projected in Year 3. One is related to stretch-steering of TuFF tape to reduce the MSR and the second is a project to develop a computational method to predict buckling loads of panels with steered tape paths.

UD-CCM's LA-AFP Mikrosam system

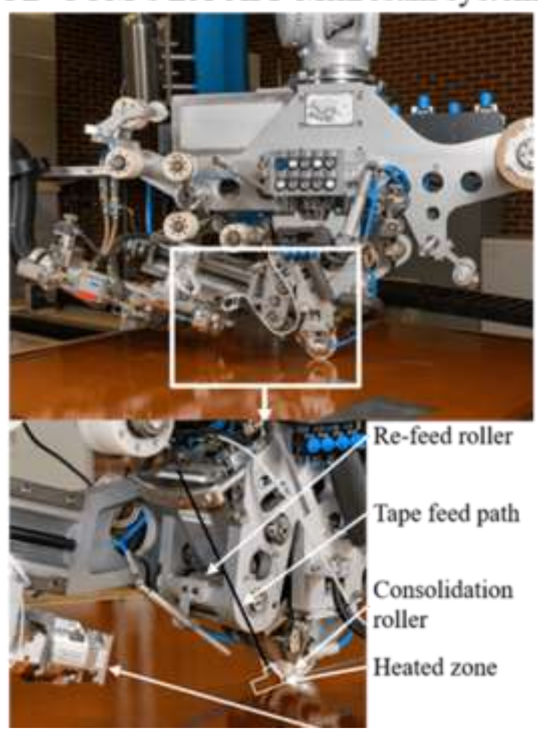

Stretch-Steering of TuFF Tapes

This study utilizes 57% fiber volume fraction TuFF tape comprised of thermoplastic Polyetherimide (PEI) matrix with 3 mm long IM7 carbon fibers. The Laser-Assisted Automated Fiber Placement (LA-AFP) process is used to study the limits of stretch-steering of TuFF tape at small radii.

An experimental technique based on photogrammetry was developed to quantify the effect of stretch parameters on the tape strain fields and path placement accuracy. The measurements captured the local in-plane strain tensor (longitudinal, transverse, and shear) across the width and along the length of steered tapes. The results demonstrate that placement path accuracy can be achieved when the tool center point (center of rotation) of the AFP head is located at the nip-point versus the roller centerline typically used for steering continuous fiber tapes at large steering radii.

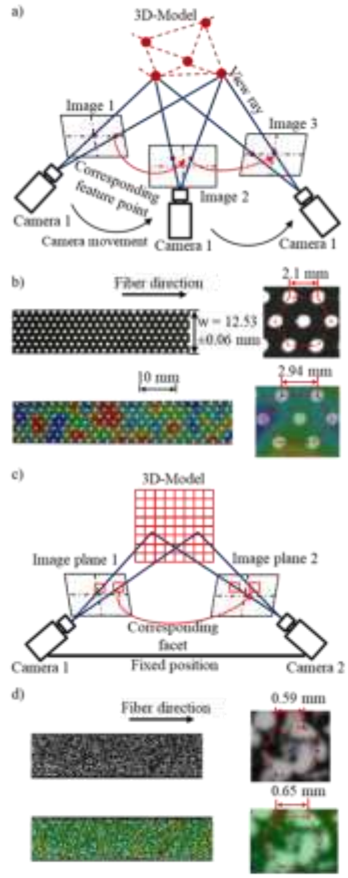

(a) *Schematic of the measurement principle for photogrammetry,*
(b) *(b) Point grid before and after stretching with 40% applied strain,*
(c) *(c) Schematic of the measurement principle for DIC strain measurement,*
(d) *(d) Speckle patterning before and after stretching with 10% applied strain*

Accuracy of the in-situ tape stretching was demonstrated up to 60% applied strain where excellent agreement between DIC and photogrammetry was achieved.

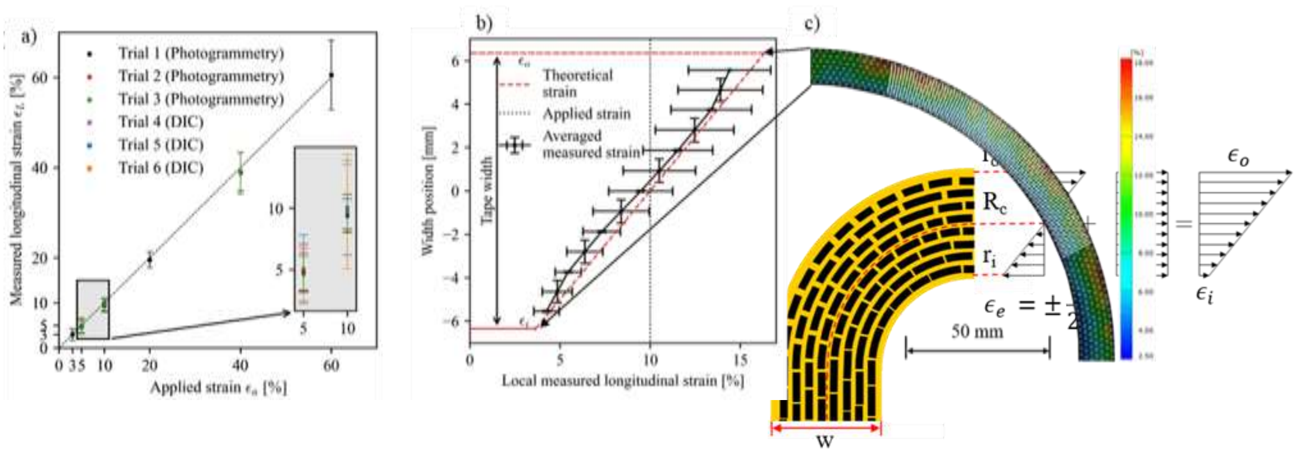

The measurements also confirm that when stretch-steering Tuff tape, the resulting strain across the tape width is the superposition of the in-situ applied tensile strain and in-plane bending computed from the tape width and steering radius.

A statistical-based methodology is presented to select the average tensile stretch levels with a suitable safety factor to minimize probability of defects forming during steering. Our experiments show that a 12.5 mm wide TuFF tape can be accurately placed on a 50 mm radius of curvature without defects. This represents an order of magnitude improvement in steerability over continuous fiber tapes of the same width.

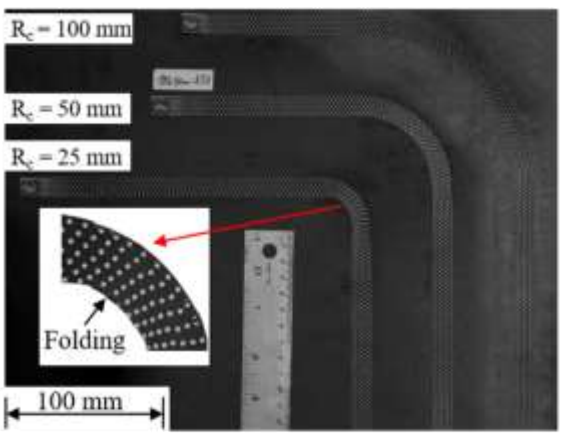

Steering of 12.5mm TuFF PEI tape at 100, 50 and 25 mm steering radius with applied tensile strains of 10, 18 and 32%, respectively.

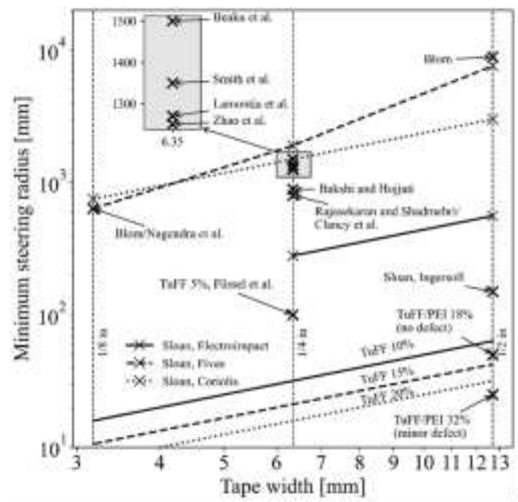

Minimum steering radius from different studies

Analytical Buckling Analysis for Tow-Steered Laminates

Automated fiber placement techniques have allowed the manufacturing of tow-steered composites which have demonstrated higher buckling strength and greater weight saving potential compared to traditional straight fiber composites. This is due to curving the fibers within a ply, tailoring the elastic stiffness of the composite. In previous work done by Tatting and Gurdal, the effect of tow-steering around a hole has been studied and a procedure for designing and analyzing finite element models for tow-steered composites has been developed. Now, an analytical procedure for the buckling analysis of tow-steered composites is desired since analytical models are computationally cheaper than finite element models. Through NASA's University Leadership Initiative (ULI) program, the University of Delaware Center for Composite Materials (UD-CCM) has been able to send a University of Delaware graduate student (Eli Bogetti) to NASA to help develop an analytical mode to predict buckling of tow-steered composites.

The Rayleigh-Ritz formulation of the buckling problem was initially programmed in Mathematica to predict a plate's buckling loads and corresponding modes. While the results matched those found in literature for isotropic plates, a shorter computation time was sought before testing anisotropic plates and implementing tow-steering. The program was therefore translated into python which showed to be match the initial program and the literature results with a much quicker computation time.

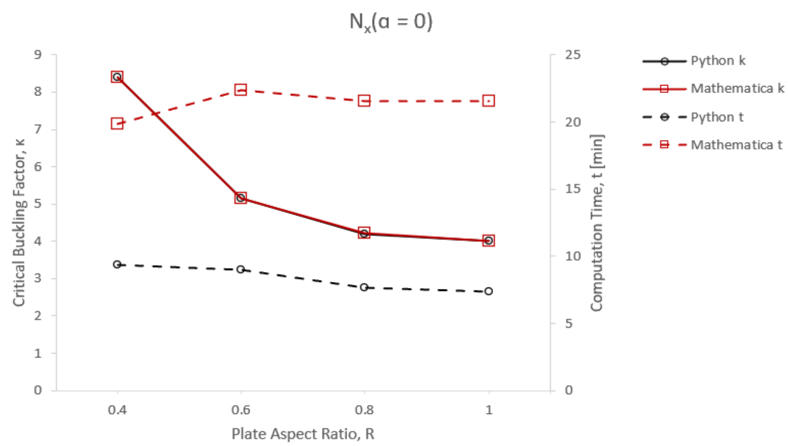

Comparison of non-dimensional buckling factor between Mathematica and python program for a plate under constant uniaxial loading, $N_x(\alpha = 0) = N_{crit}\left(1 - \alpha \frac{y}{b}\right)$, with different aspect ratios.

With the computation time reduced, testing of the anisotropic case has begun as well as an initial implementation of tow-steering. It is anticipated that the tow-steered plates may exhibit both local coupled and uncoupled regions within the plate. For the anisotropic case, the selection of the assumed in-plane and out-of-plane displacement functions is of more importance, and the effects of these assumptions on the predicted buckling behavior are also being studied. The displacement functions, u, v, and w, need to be able to capture the full effect of any elastic coupling present. The out-of-plane deflection function, w, unlike the in-plane displacement functions, also needs to satisfy the boundary conditions of the plate.

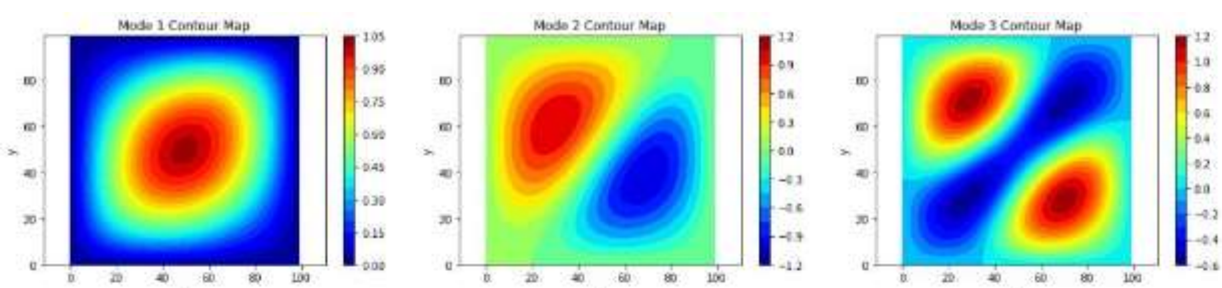

Predicted first three modes of a simply supported graphite/epoxy $[0_2/30_2/45_2]$ *laminate under constant uniaxial loading.*

During Eli's time at NASA, he worked under his mentor Brian Mason and with Erin Anderson, Andrew Lovejoy, and the rest of the ISAAC team. He got to observe the ISAAC robot and see how his project fits into the larger project. With help from his mentor, he got a better understanding of how the ISAAC team was looking to implement tow-steering and a description of the paths used. Currently, the tow-steering formulation has been programmed and implemented in the determination of the ABD matrices but has not been incorporated into the buckling problem yet.

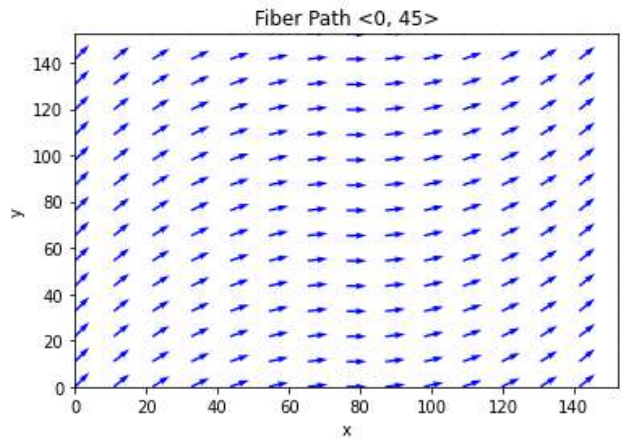

Example of the implemented linear tow-steering path for a $< T_0, T_1 > = < 0, 45 >$ *ply, where* T_0 *is the fiber angle at the center of the ply and* T_1 *is the fiber angle at the ply edges.*

Highlights: Micromechanics of Aligned Short Fiber Composites

To study the dynamics of a single fiber tensile break within a composite and the associated effects of stress wave propagation in the fibers, interface and matrix, a 3D micromechanical Finite Element (FE) model with a hexagonal packing of parallel fibers is developed. The effects of a dynamic fiber break on energy dissipation associated with resin plasticity and interface debonding using cohesive traction laws are included. The 3D FE model also incorporates process-induced residual stresses that induces radial compression at the fiber-matrix interface due the mismatch in CTE and Poisson's ratios between the fiber and matrix. During dynamic fiber failure where interface debonding occurs, radial compressive residual stresses lead to additional frictional energy dissipation in the debond region of the interface. A map of the dynamic stress concentration factor (SCF) values on the surface (along the axial as well as circumferential directions) of the fibers which are neighboring the fiber break is generated. A stability criterion based on an energy balance between elastic strain energy released by the fiber and energy

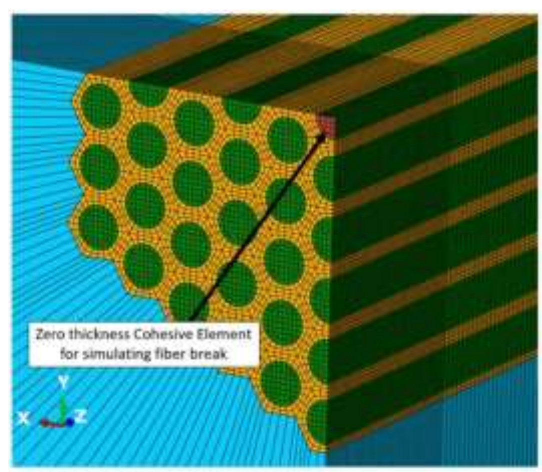

3D FE model with hexagonal packing of fibers.

dissipation (resin plasticity, interphase debonding and frictional sliding) is established to predict maximum fiber strength that initiates unstable debonding of the interface characteristic of axial splitting of the unidirectional composite loaded in tension. The FE modeling results also indicate that the dynamic fiber break introduces strain rates on the order of 10^6/s in the fiber and matrix, and up to 10^{12}/s in the interphase. This model will be combined with the defect map (reported in Year 2 Annual Report and included in the list of publications) for surface defects to predict tensile strength of unidirectional composites in the coming year.

The 3D model has unique features compared to 2D dynamic fiber break models in the literature:

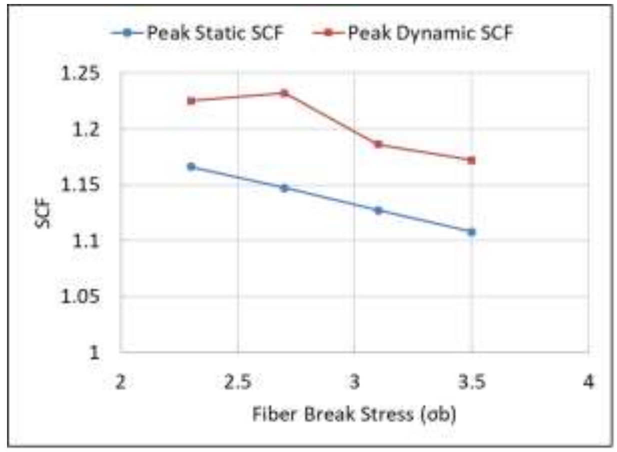

Dynamic vs Static Peak SCF values in nearest neighbor fiber

1. There are six nearest neighbor fibers adjacent to a broken fiber which take up the majority of the stress concentrations, as opposed to the 2D model which had only two nearest neighbor fibers accompanying a broken fiber.
2. The actual cylindrical geometry of the fibers is captured in the 3D model, whereas in the 2D models, the fiber and matrix regions were modeled as rectangular slabs of unit thickness.
3. The 3D model captures the residual stresses in the composite microstructure caused during the cooling down of the composite post-cure due to the mismatch in coefficient of thermal expansion (CTE) between the fiber and the matrix. The 2D models could not capture these residual stresses owing to the simplified geometry used.
4. The 3D model also captures the additional stresses created within the microstructure due to the mismatch in Poisson's ratio of the fiber and the matrix. In the 2D models, these effects were not accounted for. The 3D model also captures circumferential gradients in the stress concentrations in the fibers neighboring a break.
5. The 3D model captures frictional energy dissipation associated with interfacial debonding.
6. The 3D model enables a more realistic stability criterion for interface debonding including energy dissipation mechanisms from friction, interface debonding and matrix plasticity. This criterion provides an upper bound on fiber tensile strength that can be achieved in the composite.

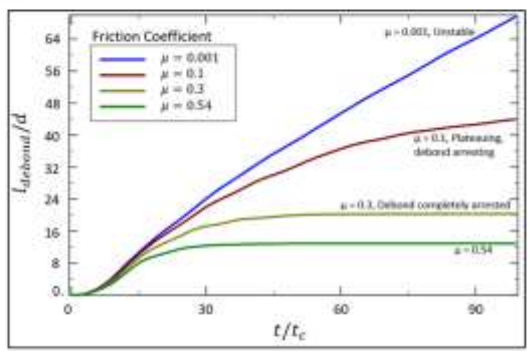

Debond growth vs. Time for elastic matrix with various coefficients of interfacial friction. The dynamic FE model simulation is stopped at t=165ns since the stress waves reach the boundary of the discretized domain.

Highlights: Micro-Mechanics: Fiber Waviness Development

The motivation for this years' study was to understand thin ply effects of transverse cracking in cross-ply LM-PAEK laminates. In last years' annual report, it was shown that the S-N curve for unidirectional 3mm IM7/LM-PAEK laminates was equivalent to continuous fiber composites due to the excellent fiber-matrix adhesion high toughness of the matrix. In Year 3, 3mm [0/90/0] IM7/LM-PAEK TuFF cross-ply composite specimens were prepared. The TuFF panels were prepared using an autoclave under a vacuum bag with an applied pressure of ~2 MPa and then cooled down from 380˚C to room temperature. Panels were C-scanned to confirm quality was achieved. Cut samples were then carefully polished and cross-sections were viewed using Keyence VHX 6000 optical microscope. Using the microscopic images along the length of the specimen, the max angle of the most severe waves of fiber (see Table below), significant layer waviness was observed. Fatigue studies as reported later were conducted on the laminate with the thickest 90 layer (240 gsm) to study transverse crack evolution for the first time. However, our past work on the origin of fiber waviness in single fiber model composites was extended to identify the mechanism and solution for reducing layer waviness.

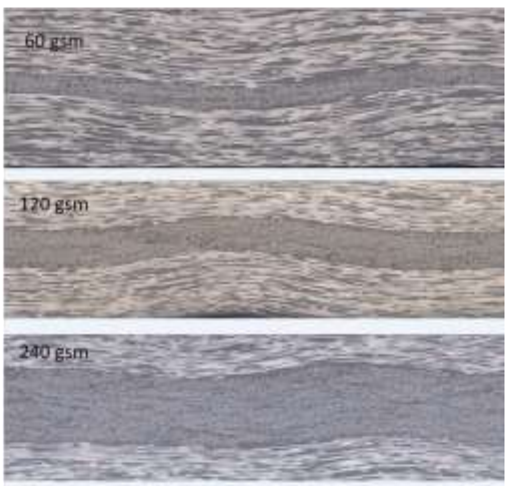

Most severe waves of fiber near the 90˚ layer with thicknesses ranging from 60 gsm to 240 gsm

Waviness Parameters

Cross-ply areal Weight	Amplitude	Wavelength	Max angle
gsm	µm	µm	deg
240	32	1152	9.7
120	34	1375	8.8
60	34	1294	9.4

Fiber waviness in fiber reinforced composites leads to higher variability and a reduction in the material’s strength and stiffness. The key parameter is the maximum out of plane angle where higher angles can trigger interlaminar shear related failures. Last year’s novel micro-mechanical visualization studies conducted on polypropylene highlighted fiber waviness develops during the amorphous melt phase and not during crystallization (if applicable for the resin). Also, the results indicate that two important processing variables that influence fiber waviness development in thermoplastic carbon fiber composites. First, adequate resin viscosity at around 40,000 P is a level of viscosity sufficient to stabilize the fiber from moving in the transverse direction, thus preventing waviness formation. Second, a large process ΔT, in the range of 80 °C or greater beyond the crystallization temperature, results in more severe waviness. By reducing the process temperature, waviness can be mitigated.

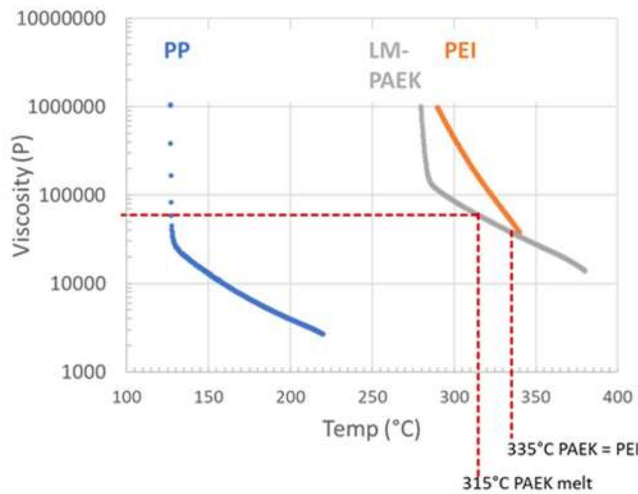

Following these insights from the model polypropylene material, a select few experiments have been conducted utilizing LM-PAEK. The select temperatures and corresponding viscosities are shown in the following figure. The highest process temperature of 380°C results in a wavy fiber consistent with the layer waviness in the cross-ply laminates above. When the process temperature is lowered to 335°C (where both viscosities of PP and PEI are sufficient to prevent waviness formation) there is no waviness formation. Further lowering the process temperature to 315°C also results in a straight fiber.

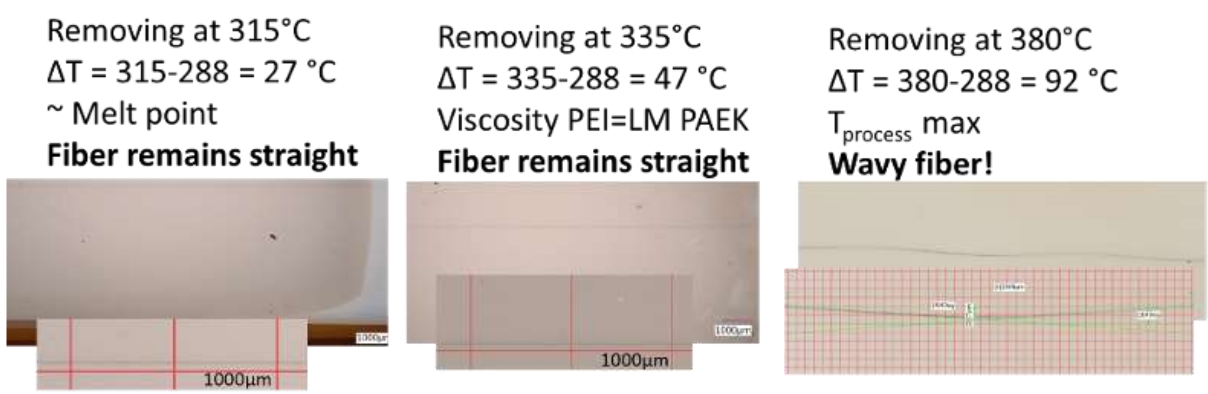

(a) (b) (c)

However, an important consideration for semi-crystalline thermoplastic composites is to erase the thermal history. Differential scanning calorimetry (DSC) of the LM-PAEK polymer indicates at 315°C melting is not complete. The DSC cooling curve of the polymer processed at 315°C shows a small peak before the onset of the primary crystallization. This is an indication that the polymer crystals have not fully melted at 315°C and act as nucleation points for crystal growth. This feature is not shown in any of the specimens processed at a higher temperature. Utilizing the combination of micro-mechanical visualization and DSC techniques we have identified a process window for panel-scale laminate production in our autoclave process.

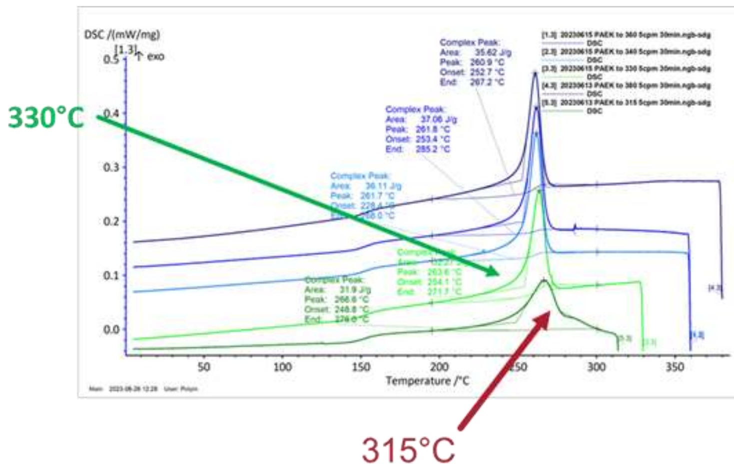

Observations from the single fiber LM-PAEK experiments will be implemented in panel/ply-scale processing runs in the autoclave to achieve waviness-free composite panels with less variability in strength.

Simulation Results

In the past year, we have formulated a first-generation model to predict the buckling of a single fiber in an amorphous viscous polymer subjected to cooling. It is our intent to validate the model predictions with the single fiber experiments mentioned above and to use the model for process optimization.

The fiber bending in cooling and contracting highly viscous fluid is shown schematically in this figure.

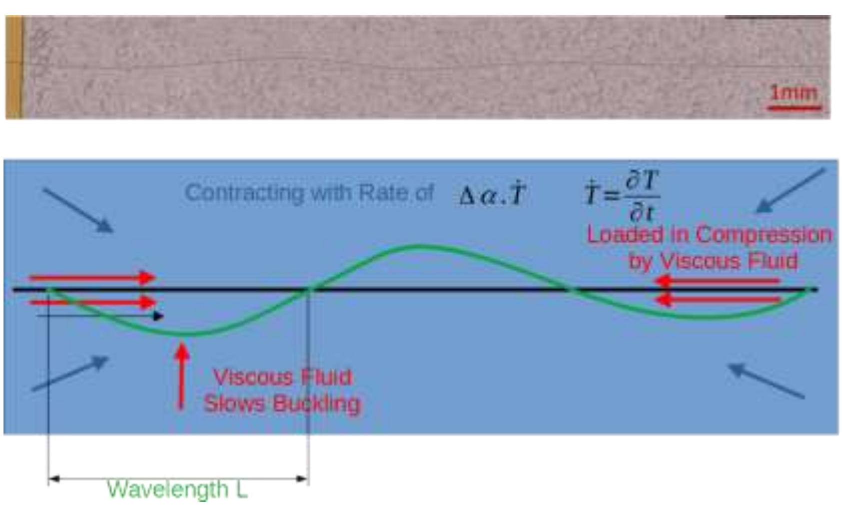

Forces and Geometry of Fiber Bending in Contracting Fluid

The fluid, having a higher coefficient of expansion than the fiber in the axial direction, flows around fiber and loads it in compression through shear stress acting on the fiber surface. This may lead to buckling, though the deformation is *not instantaneous* as the viscous flow also resists fiber bending (transverse deformation) that is proportional to axial contraction and bending rate (creeping flow is assumed).

First Order Scaling Analysis

To determine the factors that influence the presence or absence of deformation, scaling analysis of the problem is the first step. Generally, in beam buckling.

$$F_{crit} = C_{crit}\,(EI)/(L\text{^}2)$$

Where L is characteristic wavelength and EI is the bending stiffness of fiber. Based on the single fiber experiments, the length of the fiber is approximately 30mm. However, current experiments are exploring the effect of fiber length on the buckling response. Uncertain of support boundary conditions, we can only estimate that C_{crit}~1.

We can estimate the force in center of the fiber based on half its length which may cover *N* wavelengths:

$$F_{crit} \sim \eta\,.\,\Delta\alpha\,.\,\dot{T}\,.\,(N.L)^2 = \eta\,.\,\Delta\alpha\,.\,\dot{T}\,.\,L_{total}^2$$

Thus, the critical load for given buckling length *L*.

$$\left(\Delta\alpha.\dot{T}\right)_{crit} = C\,\frac{EI}{\eta L^2 L_{total}^2}$$

Which can estimate the buckling length *L* based on known contraction parameters.

$$L = \sqrt{\frac{C.EI}{\eta\, L_{total}^2\, \Delta\dot{\alpha}T}}$$

Now, the issue is that *the wavelength* depends on bending stiffness, axial contraction rate and viscosity. The latter is changing *with time*. Generally, the buckling length will decrease as the cooling progresses, the length eventually becoming of interest (in mm).

Based on this scaling analysis, the buckling (or bending) in viscous environment is *inevitable*. We do not observe that experimentally. The reason is that the deformation has to develop with limited speed. Any off-axis bending deformation of fiber is opposed by viscous force as the fiber moves through viscous fluid. This force *will also depend on viscosity. Recall our experiments show that a critical viscosity stabilized the fiber form transverse bending/buckling.*

Should we describe the deformation by rotation φ at the fiber stationary points (with rate $\dot{\varphi}$), the reaction load *R/L* (per unit length) that slows down buckling is:

$$R/L \sim C_2\, \eta\, L\, \dot{\varphi}$$

C_2 is another proportionality coefficient (assumed to be or order one). Meaning the higher the viscosity and the longer the wavelength, the slower the rotation and bending progresses. In this case the scaling estimate of *what* will happen and how the deformation develops is not easily available, and impossible if viscosity is transient (temperature dependent). To obtain proper description, one needs to resort to numerical modeling.

Numerical Implementation

Assuming symmetry in the mid of the fiber, the problem can be described as shown below.

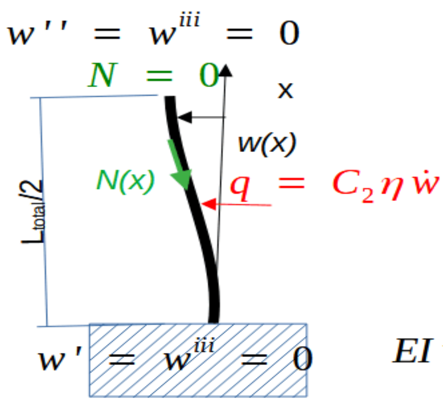

N Integrated from End:

$$N' = C_1 \eta(t) \dot{T} \Delta\alpha\, x$$

$$N = -\frac{C_1 \eta(t) \dot{T} \Delta\alpha}{2}\left(\left(\frac{L}{2}\right)^2 - x^2\right)$$

$$EI\, w^{iv} + \left(\frac{C_1 \eta \dot{T} \Delta\alpha}{2}\left(\left(\frac{L}{2}\right)^2 - x^2\right) w'\right)' + C_2 \eta \dot{w} = EI w_o^{iv}$$

The problem is described as linearized, with transient values for contraction and resin viscosity. The fiber buckling problem governing equation(s) are given. Note that absolute value of displacement w is evaluated from horizontal equilibrium.

The governing equation does not offer “nice” closed form solution. The approach is to:

- Discretize the fiber length and the equation.
- Explicit or semi-implicit form is possible. We chose the latter with *w* being solved implicitly as it provides sizeable time step.
- Slight shape disturbance is applied to fiber.
- The equation is marched in time until the process is finished or buckling (sizeable deflection) occurs.

The model was tested for constant viscosity and modeled contraction period long enough to buckle the fiber for given cooling rate. The Parameters were E=200 GPa, fiber diameter 0.005 mm, L_{total}=30 mm and the drag coefficient C_1 and C_2 being 1. Viscosity was set to 10000 Pa.s.

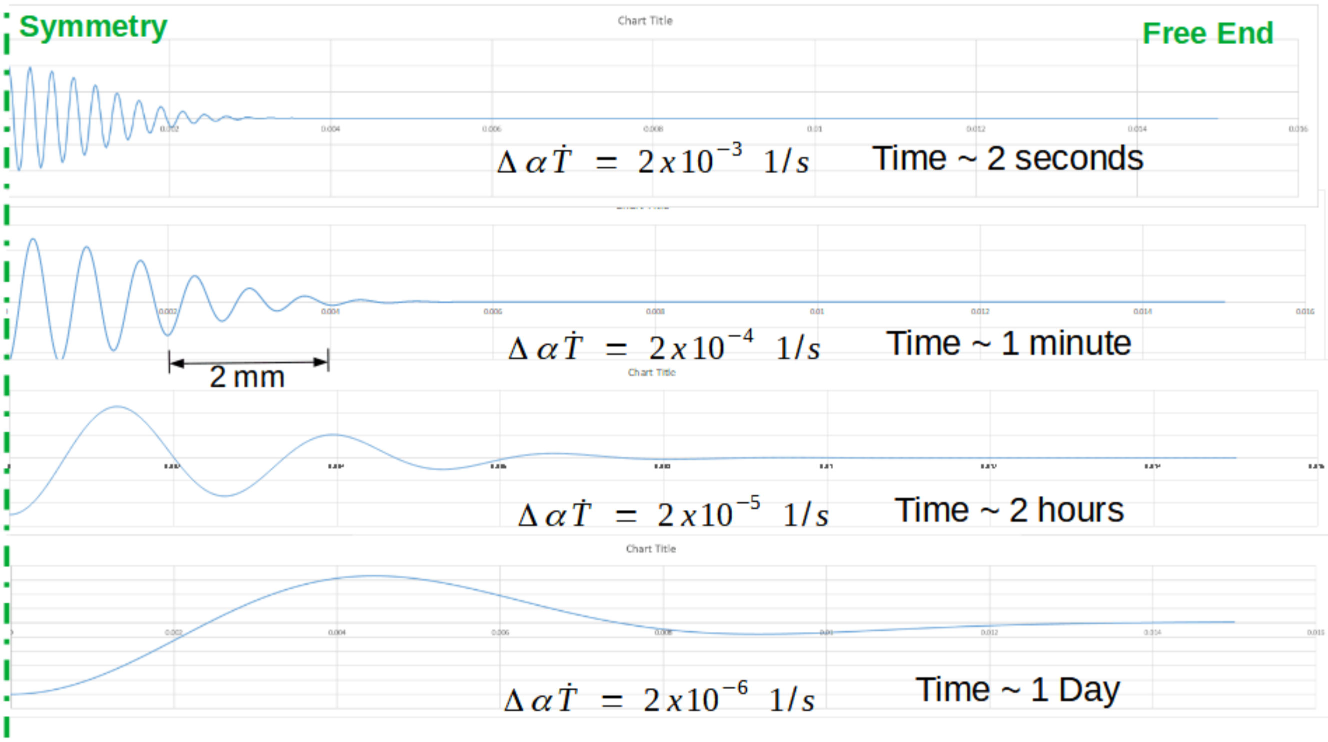

Fiber buckling shape and time based on the rate of cooling: Viscosity constant.

Note that the usual values for cooling rate in the experiments are $\Delta\alpha\dot{T} = 1x10^{-4} \sim 1x\ 10^{-6}\ 1/s$ and time span of hour but the viscosity is lower over much of this time. Future work will incorporate more realistic temperature dependent viscosity for both polypropylene and LM-PAEK and study the effects of increased fiber length on the predictions. The model predictions will be compared to the new experimental data being generated.

Highlights: Process-Induced Residual Stress in Semicrystalline Thermoplastic Composites

Most of the literature assumes temperature-independent matrix properties to calculate the residual stress developed in the composite. The simplest approach to predicting residual stress is to assume a stress-free temperature (T_{sf}) and use the constituent materials' CTEs to calculate the thermally induced stress and strain state (Approach 1 in Figure). In many thermosets and amorphous thermoplastics, T_{sf} is approximated by T_g. This method may lead to inaccurate residual stress predictions because temperature-dependent material properties and crystallinity shrinkage are not accounted for. This approach applied to semicrystalline PP (T_g of 0°C) would incorrectly predict the composite residual stress at room temperature.

A second approach, reported in our previous studies (reported in last years' annual report) on residual stress in semicrystalline polymers, assumes T_{sf} is the temperature at the end of crystallization (cooling rate dependent) recognizing that the presence of a crystalline phase is capable of carrying stress at temperatures above T_g. The general trend is that crystallization starts at a higher temperature (i.e., higher T_{sf}) during slow cooling and starts at a lower temperature during fast cooling (i.e., lower T_{sf}). This has led to T_{sf} being defined as a function of cooling rate using the polymer crystallization kinetics. In these models, residual stress calculations have used both temperature-independent modulus and temperature-dependent modulus (at equilibrium crystallinity) and CTE only. The contribution of crystallization shrinkage is assumed negligible in these studies. Experimental validation of this modeling approach has been limited.

In our Year 3 work, a comprehensive model for residual stress is developed without making any of the simplifying assumptions reported in the literature. The material model for the matrix, needed for predicting residual stress, starts in the amorphous polymer melt (stress-free) and includes the effects of non-isothermal crystallization kinetics down to room temperature (T_{RT}). The material models include the effects of crystallinity on temperature-dependent matrix modulus and matrix shrinkage from both thermal and crystallinity (Approach 3 in Figure 1). No assumptions related to stress-free temperature are made in this model. The contributions of crystallization shrinkage on residual stress are also included.

Flowchart for calculating thermal residual stress (T_g = Glass transition temperature and T_{RT} is room temperature). Approach 3 is developed in this paper.

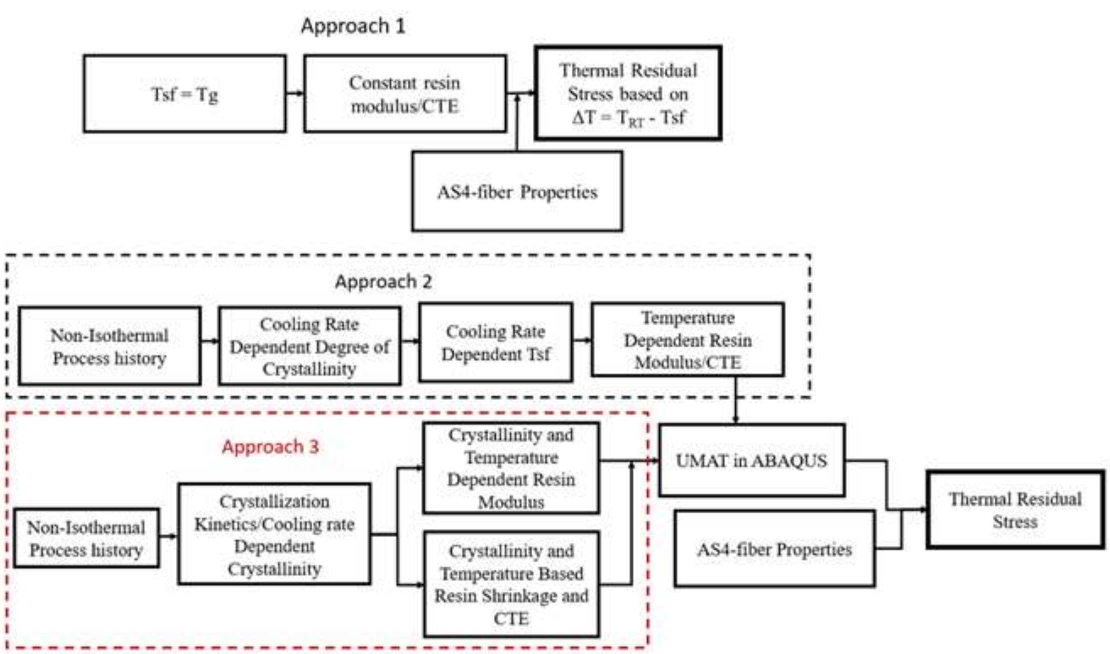

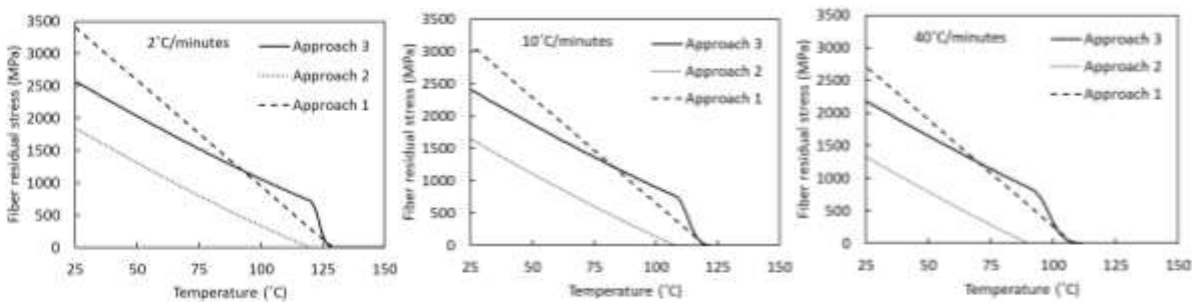

(a) (b) (c)

Axial residual stress at the mid-length of the fiber from T_m to T_{RT} (a) 2˚C/minutes (b) 10˚C/minutes and (c) 40˚C/minutes. All stresses are compressive.

The percent error of the residual stress at T_{RT} for Approach 1 and 2 compared with the more accurate Approach 3 developed in this study. Approach 1 provides overestimate residual stress by 24-32% (a positive error corresponds to compressive stress greater than Approach 3). Approach 2 underpredicts residual stress by 28-39% (negative error corresponds to compressive stress less than Approach 3).

	2˚C/minutes	10˚C/minutes	40˚C/minutes
Approach 1	24 %	29 %	32 %
Approach 2	-28 %	-32 %	-39 %

Similar errors in Approach 1 and 2 are found when the residual axial strain along the entire length of the fiber (mid-length to free surface) for the thermal history of thin film single fiber composite with preload of 4 g (pre-strain of 0.43%). Recall from last year's annual report that predictions of axial strain in the AS4 carbon fiber were validated using Raman spectroscopy.

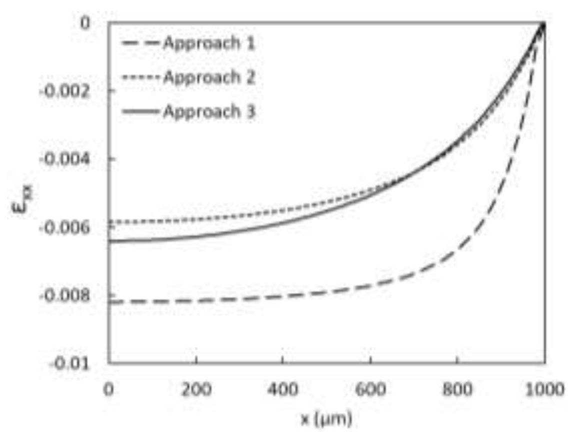

Highlights: Fatigue Performance of Highly Aligned Short Fiber IM7/LM-PAEK Thermoplastic Composites

Tailorable universal Feedstock for Forming (TuFF) is a highly aligned short fiber composite material (fiber aspect ratio of 600) that can achieve a high fiber volume fraction (50-60%). The studies on unidirectional (UD) 3mm IM7/polyetherimide (PEI) have demonstrated quasi-static and tension-tension fatigue properties comparable to continuous fiber composites (57% fiber volume fraction). In previous years, UD 3mm IM7/Low-Melt Polyaryletherketone (LM-PAEK) TuFF panels (Vf = 54%) were tested in the fiber direction using a tensile fatigue methodology to generate an S/N curve (R = 0.1, 3 Hz) with periodic checks for modulus loss over a minimum of 1 million cycles. The results indicate 3mm IM7/LM-PAEK is superior to other discontinuous fiber composites and equivalent to other continuous fiber composites in the literature. The comparison is based on the slope of normalized strength versus cycles on a semi-log plot with LM-PAEK exhibiting the lowest slope/strength reduction. No reduction in axial fiber tension modulus was measured.

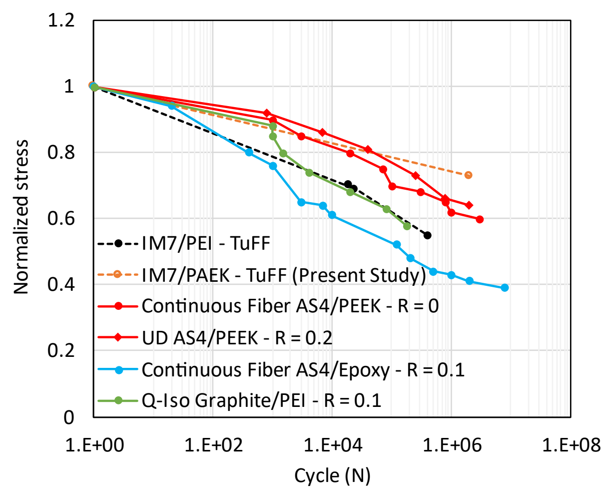

This year's work further looks at the tension-tension fatigue performance of [0/90/0] IM7/LM-PAEK TuFF cross-ply laminate with a thick ((240 gsm) 90˚ ply subjected to a maximum tensile strain of 0.9% (R = 0.1, 3 Hz). Typically, cross-ply composite layups exhibit transverse cracking in the transverse plies (90˚ layer) that extend across the entire thickness. Models and experimental studies show that the initiation and saturation of transverse cracking during static loading depend on several factors including mechanical loading, residual stress, and ply thickness. The effect of fatigue loading has been shown to reduce the initiation strain. In general, initiation strain for transverse cracks decreases with increases in residual stress and ply thickness (the typical range of initiation strain is 0.1 to 0.6% tensile strain as shown below for continuous fiber IM7/K3B cross-ply laminate). The key material property at the continuum length scale governing transverse cracking is the intralaminar fracture toughness of the 90˚ layers.

In the present study, the thickest [0/90/0] (240 gsm) in the cross-ply 3mm IM7/LM-PAEK TuFF laminates exhibited no transverse micro-cracking up to ~1.5 M fatigue cycles with a 0.9% maximum strain (R=0.1, 3Hz) as shown in figure 3. In comparison, this significant level of applied max strain (0.9 %) with no micro-cracking is ~50% higher than the initiation strain level for a typical carbon/epoxy having a much lower intralaminar fracture toughness (initiation strain is 0.6% and exhibits crack saturation (24 cracks/cm as shown in Figure 4). The high degree of fatigue damage resistance observed for the 3mm IM7/LM-PAEK TuFF is attributed to the significant level of interface adhesion between the fiber and the resin (Interfacial Shear Strength of 120 MPa) and high matrix ductility (>40% strain to failure) and high intralaminar fracture toughness of the 90˚ layers.

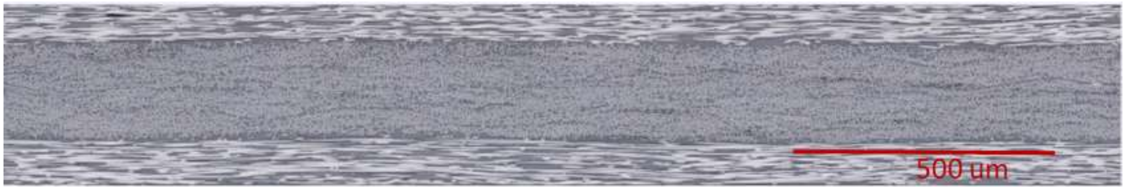

Cross-section of [0/90/0] IM7/LM-PAEK TuFF cross-ply laminates with a thick 90˚ ply areal weights of 240 gsm. No transverse cracking is observed after fatigue at 0.9% (R=0.1)

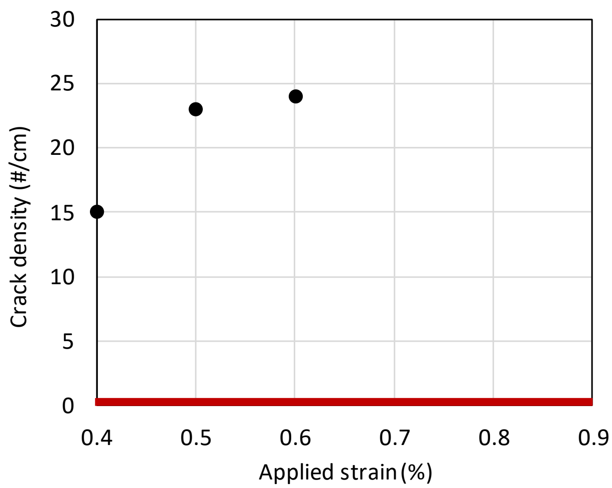

Matrix crack density in 90° plies of [0/90/0] laminate at ~1 million cycles. Continuous IM7/K3B (black dots) exhibits a crack density of 25/cm. In comparison, 3mm IM7/LM-PAEK cross-ply (red squares) exhibits zero crack density (does not microcrack at strains less than 0.9% strain). Our plans for the coming year will focus on fatigue testing of the cross-ply laminates with reduced ply thickness (once the process has been optimized to reduce layer waviness) at higher strain levels.

Highlights: Investigating Interfacial Healing Performance of IM7 Single Fiber Reinforced Multifunctional Vitrimer Composite

Obed Tetteh, a graduate student at Southern University (SU) visited the University of Delaware-Center for composite materials (UD-CCM) in January and June of this year where he is working on self-healing interfaces.

This project is being conducted together with Mr. Munetaka Kubota under the supervision of Professors Gillespie Jr. and Li. Low-velocity impact scenarios can cause interlaminar and fiber/matrix debonding in fiber-reinforced polymer composites. Self-healing of these interfaces can potentially elongate the service life of these components. A previous study by Feng and Li used a self-healable vitrimer diglycidyl 1,2-cyclohexanedicarboxylate (DCN)/branched polyethylenimine (PEI) showed the ability of these low glass transition temperature (T_g) vitrimers to self-heal within a laminate.

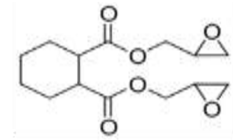

Diglycidyl 1,2-cyclohexanedicarboxylate
Mw: 284.31 g/mol

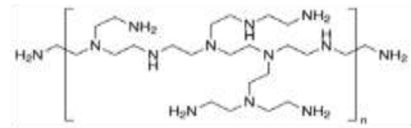

Branched Polyethylenimine M_w ~800 g/mol

This study explores the characterization of the fiber/matrix interface and developing a method to characterize the self-healing efficiency for a DCN/PEI with a higher T_g for potential structural applications. In this study, a 3:1 DCN:PEI formulation was chosen for its higher glass transition temperature (94°C) as compared to the 1:1(41.6 °C) developed by Feng and Li in 2021. A method to make fiber pullout samples using unsized Hexcel IM7 with a 3:1 DCN:PEI ratio was developed, and preliminary data was collected for the effective interfacial shear strength (IFSS) between IM7 and the DCN/PEI self-healing vitrimer last year.

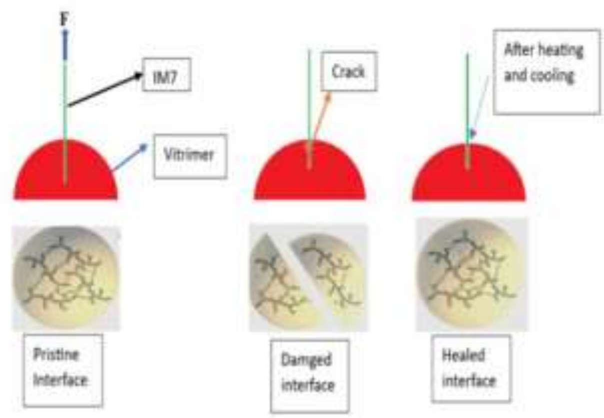

This year more replicates were made using the process as shown, some representative force-displacement curves are shown in figure below to gain a better insight into the failure modes of the fiber/matrix interface which resulted in an IFSS of 95 MPa, exceeding the minimum IFSS (50-60 MPa) required for direct property translation in TuFF-based composites. To measure the healing efficiency of the fiber/matrix interface, it is required to develop a process that allows the resin to relax and establish intimate contact with the failed surface and allowed to heal. Self-adhesion is required during the healing of the debonded interface.

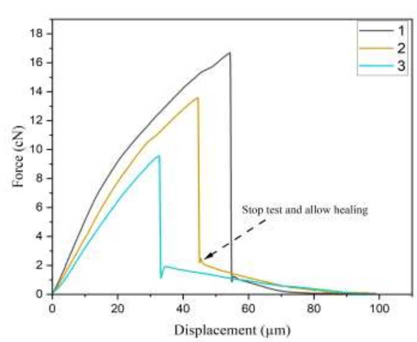

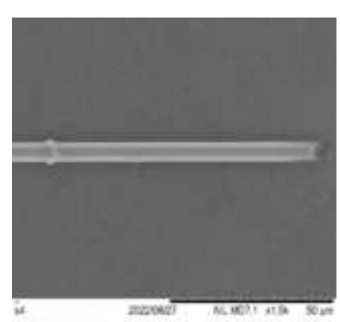

Stress-relaxation experiments were conducted to investigate the malleability and kinetics of the bond exchange reactions. These bond exchange reactions are crucial for self-healing. Furthermore, lap shear tests were also conducted to verify the self-adhesion/weldability of the vitrimer. The minimum vitrification temperature (T_v) required for bond exchange reactions in the shape memory vitrimer was found to be 160 °C, which would promote self-healing. Based on the T_v, temperature-dependent stress relaxation tests were conducted at different temperatures (160, 170, 180, 190, and 200 °C) to characterize the malleability and kinetics of transesterification. The vitrimer exhibited a relatively faster relaxation time, and the characteristic relaxation time decreased with increasing temperature, as shown below. Lap shear tests were conducted to investigate the weldability and adhesion strength of the vitrimer and gave confidence in the proposed self-healing process conditions. The samples were welded at different temperatures with varying overlap lengths under 450 kPa pressure. The samples welded at 170 °C with an overlap length of 10 mm under a welding pressure gave a good adhesion strength (2.26 MPa.. The welding performance can further be increased by increasing the welding time. From these results, the self-healing temperature and pressure for the healing interface experiments were determined as 170 °C under 450 kPa.

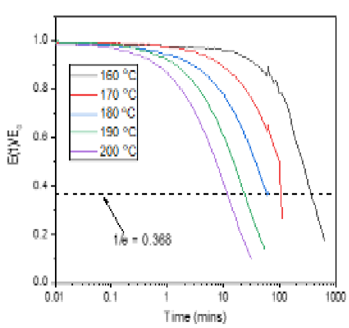

Healing single fiber pullout tests under 170 °C for 4 h at 450 kPa without damaging the sample is challenging due to the sample geometry and how fragile single filaments of carbon fiber can be. To apply precise temperature and pressure, the high-pressure DSC (HP-DSC) will be used. Preliminary tests were conducted to confirm the sample will be unharmed during the pressurization step, showing the fiber remained intact even after exposure to turbulent pressurization conditions. The initial fiber pullout tests required for the self-healing interface experiments will be conducted using a custom Instron 5944 MicroTester as shown below. The next step is to capture a partially tested sample, stopping at the indicated position and place it into the HP-DSC to heal, and retest the fiber pullout specimen till failure to determine the healing efficiency. Laminate level healing will also be investigated by measuring interlaminar toughness in modes I, II, and mixed-mode and repeating after healing in the coming year.

Papers/presentations

1. Legenstein, A. Fussel, L., Heider, H. Gillespie Jr. J. W., Center T. A. “Stretch-Steering of Highly Aligned Discontinuous Carbon Fiber Tape with Automated Fiber Placement, Composites Part B, August 2023.
2. Parambil, Nithin K. Chen, B.R.,Gillespie Jr, J.W., “Process-Induced Residual Stress in a Single Carbon Fiber Semicrystalline Polypropylene Thin Film, submitted Composites Part A, July 2023.
3. Fuessel, Lukas, Cender, T., Gillespie, Jr., J.W., “Influence of Deformation of Complaint Rollers on Tape Steering During Automated Tape Placement”, ASC Conference, University of Masachusetts, https://www.asc-composites.org/ascc2023 , Sept. 17-20, 2023
4. Parambil, Nithin K., Chen, B.R., Gillepsie, Jr., J.W., “Fatigue Performance of Highly Aligned Short Fiber IM7/LM-PAEK Thermoplastic Composites”, ASC Conference, University of Masachusetts, https://www.asc-composites.org/ascc2023 , Sept. 17-20, 2023
5. Chen, Branndon R., Parambil, N.K., Deitzel, J.M., Gillespie, Jr., J.W., “Micro-Mechanical Investigation of Process-Induced Fiber Waviness in Thermoplastic Composites” ASC Conference, University of Masachusetts, https://www.asc-composites.org/ascc2023 , Sept. 17-20, 2023
6. Cender, Thomas, Simacek, P., Gillespie, Jr., J.W., Advani, S.G., “Experimental Characterization of Extensional Viscosity of Aligned Discontinous Fiber Composites”, FPCM-15 (15th International Conference on Flow Processes in Composite Materials), https://www.purdue.edu/cmsc/fpcm/, June 27-29, 2023
7. Legenstein, Alex, Fuessel, L., Cender, T., Heider, D., Tierney, J., Gillepsie, Jr., J.W., “Stretch-Steering of Aligned Discontinuos Fiber Tapes on Higly Curved Paths Using Automated Fiber Placement”, SAMPE 2023, https://www.sampeamerica.org/ , April 17-20, 2023.
8. Ganesh, Raja, Gillespie, Jr., J.W., “Dynamic 3D effects of single fiber tensile break within unidirectional composites including resin plasticity, residual stress, interfacial debonding and sliding friction”, *Journal of Composite Materials*, Submitted, Accepted August 2023
9. Ganesh, Raja, AbuObaid, A., Gillespie, Jr., J.W., “Novel Continuous Fiber Bending Experiment to Determine Size- and Spatial- Distributions of Surface Defects in Glass Fibers”, *Composite Science and Technology*, Vol 241, 2023, 110146.
10. Ganesh, Raja, AbuObaid, A., Gillespie, Jr., J.W., “Experimental Determination of Bimodal Strength Distribution of S-Glass Fibers”, *Composites Part B*, 2023, 110559, https://doi.org/10.1016/j.compositesb.2023.110559
11. Tetteh, O., Kubota, M. Mensah, P., Gillespie, Jr, J.W., Li G., Evaluation of the Interfacial Shear Strength, and Self-Healing of a New Im7 Single Fiber Reinforced Multifunctional Vitrimer Composite, ASME 2023 International Mechanical Engineering Congress and Exposition (IMECE2023), New Orleans, October 29-November 2, 2023

12. Featured Speaker Shridhar Yarlagadda, “Highly-aligned Discontinuous Fiber Composites (*TuFF*): Progress and Challenges, May 23-26, SAMPE 2022, Charlotte, NC.
13. Featured Speaker John W. Gillespie Jr., Nasa ULI Tech Talk Series, “Composite Manufacturing Technologies for Aerospace Performance at Automotive Production Rates”, April 18, 2022.
14. Nasa ImaginAviation, March 1-3, 2022, ULI-Aerospace Performance at Automotive Rates Featuring the University of Delaware with Taka Kubota (MSE PhD) and Steve Crimaldi
15. Nasa ImaginAviation, March 1-3, 2022, Student Sustainability Roundtable Imagining a Greener Future Featuring the University of Delaware with Uday Balaga (ME PhD) and Taka Kubota (MSE PhD)
16. Parambil, Nithin K., Chen, B., Deitzel, J., Gillespie, Jr., J.W., “A Methodology for Predicting Processing Induced Thermal Residual Stress in Thermoplastic Composite at the Microscale”, https://doi.org/10.1016/j.compositesb.2021.109562, *Composites Part B*, volume 231, 109561, 2021.
17. Simacek P., Advani S. G., Gillespie Jr. J. W., “Modeling Short Fiber Deformation in Dilute Suspension: Fiber Deposition”, https://doi.org/10.1016/j.compscitedh.2021.109149, Composites Science and Technology, volume 218, 109149, 2021.
18. Cender, Thomas A., Fidlow, H., Yarlagadda, S., Heider, D., Simacek, P., Advani, S.G., Gillespie, Jr., J.W., “Forming Limits of *TuFF* Composites in Stretch Forming Processes”, SAMPE 2022, Charlotte, NC, https://www.nasampe.org/events/EventDetails.aspx?id=1244904, May 23-26, 2022.
19. Fidlow, H., Cender, T. “Extensional Viscosity of Thermoplastic Composites in Stretch Forming Processes”, SAMPE 2022, Charlotte, NC, May 23-26, 2022.
20. Chen, Branndon R., Prakash, K., Yarlagadda, S., Gillespie, Jr., J.W., “Fatigue Performance of Thermoplastic *TuFF* Composites”, SAMPE 2022, Charlotte, NC, https://www.nasampe.org/events/EventDetails.aspx?id=1244904, May 23-26, 2022
21. Fussel, Lukas, Cender, T.A., Austermann, V., Gillespie, Jr., J.W., Heider, D., “Tow Steering of Stretchable *TuFF* Thermoplastic Tape with Laser Tape Placement”, SAMPE 2022, Charlotte, NC, https://www.nasampe.org/events/EventDetails.aspx?id=1244904, May 23-26, 2022.
22. Abu-Obaid, Ahmad, Ganesh, R., Gillespie, Jr., J.W., “Investigation of Size and Spatial Distribution of Defects in S2 Glass Fibers Using Continuous Bending Test Method”, SAMPE 2022, Charlotte, NC, https://www.nasampe.org/events/EventDetails.aspx?id=1244904, May 23-26, 2022.
23. Parambil, Nithin K., Chen, B.R., Deitzel, J.M., Gillespie, Jr., J.W., Vo, L.T., Sarosi, P., “Predicting Processing Induced Residual-Stresses in Carbon-Fiber-Thermoplastic Micro-Composites”, ASC Conference, Virtual Event, https://na.eventscloud.com/website/17366/, Sept. 19-22, 2021.
24. Chen, Branndon R., N.K. Parambil, J. Deitzel, J.W. Gillespie, Jr., L.T. Vo, P. Sarosi, “Interfacial Shear Strength (IFSS) and Absorbed Energy versus Temperature in Carbon Fiber-

Thermoplastic Composites via Single Fiber Pullout Testing," ASC 2020, https://asc2020nyc/ September 14-17, 2020.

Education/Workforce Training and Outreach Activities

UD-CCM and Southern University were actively involved in education/workforce training and outreach during the past year. More than 2,500 students were involved. The highlights include:

1) Internship Recruitment for NASA Research Centers: 19 nineteen students applied to 7 NASA sites; 2 ULI internships at NASA Langley.
2) NASA iMaginAviation Annual Conference: A gateway to Aviation Transformation
   a. 3,265 individual registrations
   b. ULI participation in Gathertown a Virtual Tour and Poster session with attendees
   c. Hosted iMaginAviation Watch Party with 50 students attending.
3) ULI co-sponsored seminar series called CCM Connects: The Future is Composites attended by 700 people.
4) ULI co-sponsored Student Achievement Day with guest speaker Dr. Steve McKnight, Director, Department of Energy Advanced Manufacturing Office.
5) Hosted Delaware Aerospace Education Foundation – Space Beam Challenge engaging 32 students (8^{th} and 9^{th} grade) in composite aerospace applications.
6) ULI co-sponsored Summer Research Symposium with over 50 participants.
7) Southern University hosted 7 events involving 8 middle schools in Baton Rouge, LA. Over 1700 underrepresented minorities were involved in these activities.
8) The details are provided in the next sections.

UD-CCM Education/Workforce Training and Outreach Activities

Recruitment of UD student for UD-CCM's undergraduate summer research program and NASA Fellowships is conducted in the spring through College of Engineering and UD's university wide Honors program. Nineteen students applied to seven NASA research centers. Two of our ULI students (Eli Bogetti and Alexander Barry) spent a summer internship at NASA Langley developing a code for panel buckling using tape steering and participating in AFP tape placement experiments. Over 40 undergraduates participated in summer projects and presented at the research symposium (details below).

Internship Recruitment for 2023
NASA Pathways (2-6-23 to 2-11-23) and Summer Internships

- Recruitment Outlets
  - UD Honors Program – university-wide
  - COE – all departments
  - CCM
    - Mail lists
    - Website Homepage
    - CCM ULI Website
    - Social Media
- Opportunities will open February 6th
- Provided is a step-by-step guide on how to create a USAJobs account and apply for positions at NASA.
- Additional information about the Pathways Program can be found in the following links:
  - https://intern.nasa.gov/
  - NASA Internship Opportunities Brochure
  - NASA Resume Tips
  - NASA Pathways Internship Program Applicant Guide

- 19 UD Students Applied
  - Mechanical
  - Material Science
  - Civil
  - Communications
  - Chemical
  - Electrical
  - Biomechanics & Movement
- Applied to:
  - Kennedy Space Center, FL
  - Langley Research Center, VA
  - Wallops Flight Facility, VA
  - Goddard Space Flight Center, MD
  - Glenn Research Center, OH
  - Marshall Space Flight Center, AL
  - Johnson Space Center, TX

NASA Contacts/Inquiries
- Jeremy Jacobs
- Sarah Luna
- Kim Daniel
- Ronald Lewis
- Karen Miller
- Steven Holz

NASA ImaginAviation (iA): A gateway to Aviation Transformation UD-CCM 2/28-3/2/2

This is an annual conference organized by NASA to promote:

1) real-time networking through engagement of NASA subject matter experts and leaders from industry and academia
2) Transformation of the future of aviation through invigorating and inspiring talks
3) STEM engagement with K-12 and university students
4) Innovation through insights provided in new technologies.

Our ULI participated extensively in iA events including iMaginAviation Gathertown, a virtual poster session and tour and an in-person student Watch Party held at UD-CCM organized by our student SAMPE chapter. The event was attended by 50 engineering students. Overall registration for the conference exceeded 3,265 individuals providing outstanding exposure to our ULI research activities and impactful experience for our student participants.

Virtual Tour and Poster Session

imaginAviation Gathertown

https://app.gather.town/app/khLBZ5Ymq6SRPN6G/imaginaviation

Our tour stop included four ULI students interacting with visitors using their posters. Additional supporting information included videos and presentations by our team members and access to our ULI website established on CCM's website (https://www.ccm.udel.edu/research/program-highlights/nasa-university-leadership-initiative-uli/)

imaginAviation Gathertown

https://app.gather.town/app/khLBZ5Ymq6SRPN6G/imaginaviation

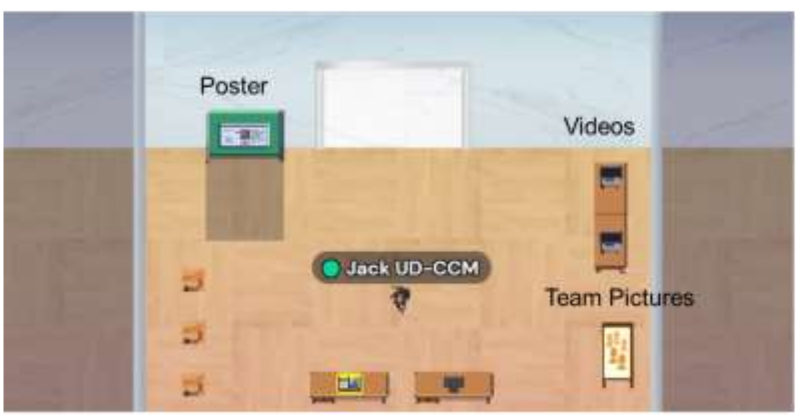

Supporting Info and Website

- Posters
- Team Pictures
- Supporting Info
  - Videos
  - Presentations
- ULI Website
- Four students online to interact with visitors
  - Taka Kubota (UD PhD MSE)
  - Obed Tettah (SU MS ME)
  - Lukas Fuesel (UD PhD ME)
  - Branndon Chen (UD PhD MSE)


Composite Manufacturing Technologies for
Aerospace Performance at Automotive Production Rates
Addressing the Technology Barriers for Urban Air Mobility eVTOL Aircraft Through Science and Innovation
National Aeronautics and Space Administration
NASA
Challenges
Barriers Addressed
CLICK FOR IMAGE FOR VIDEO
Joby TOYOTA eVTOL
Tailored Universal Feedstock (TuFF) Provides Aerospace Performance at UAM Production Rates
Expected
Innovation of Next Generation Sustainable Composites
SPIRIT
ATC
Innovation of Next Generation Composite Manufacturing
Solution
Results and Next Steps
Partners and/or Participants
5 YEARS
Joby TOYOTA
SOUTHERN UNIVERSITY
UNIVERSITY OF DELAWARE
CENTER FOR COMPOSITE MATERIALS
NASA
ULI
IMAGINAVIATION


UNIVERSITY OF DELAWARE
CENTER FOR COMPOSITE MATERIALS
Celebrating 50 Years
Composite Manufacturing Technologies for Aerospace Performance at Automotive Production Rates
ULI Research Goals
Develop Physics-Based Modeling and Simulation Tools for Aerospace/UAM Applications
Physics of fiber alignment
Microstructural design of mechanical properties
Thin-ply effects on laminate properties
Micromechanics of forming, constitutive models and forming limits
Process modeling for complex geometry parts
Experimental validation
Part Design and Manufacturing
Experimental validation (quality, repeatability)
Cost models
Creation of Property Database & Integration into Commercial Software
Composite Manufacturing Technologies
for Aerospace Performance
at Automotive Production Rates
National Aeronautics and Space Administration
NASA
Next Generation Sustainable and Self-healing TuFF Composites
Multifunctional vitrimers: Self-healing, recyclable, shape member
Highly aligned discontinuous carbon fibre preform (TuFF): Recyclable, upcyling and reuse
Obed Tettah,
SU Masters, ME
Vitrimer
TuFF
Lukas Fuessel
UD PhD student, ME
Topology Optimization by Tow Steering During AFP
Stretchable TuFF >10x Lower Radius than State of the Art
TuFF IM7 carbon (3mm) /LM-PAEK Offers Excellent Fatigue Properties
Excellent fiber/matrix adhesion
Excellent Resin Toughness Of Thermoplastics
Excellent TuFF Fatigue Properties
Brandon Chen
UD PhD student, MSEG
0.9% Tensile Strain on Cross-ply Laminate (R=0.1): 1M cycles with No Transverse Cracks
UNIVERSITY OF DELAWARE
CENTER FOR COMPOSITE MATERIALS
NASA
ULI
UNIVERSITY LEADERSHIP INITIATIVE
SOUTHERN UNIVERSITY
IMAGINAVIATION


CENTER FOR COMPOSITE MATERIALS
Composite Manufacturing Technologies for Aerospace Performance at Automotive Production Rates
Education/Workforce Training & Outreach
UD-CCM TuFF Integrated Manufacturing Facility
Principal Investigator
Prof. John W. Gillespie, Jr.
302-831-8702
ImaginAviation 2022
Taking Flight with Anderson Cooper
UD-CCM ULI Webpages
UD-CCM Website
Contact Us
CENTER FOR COMPOSITE MATERIALS
IMAGINAVIATION
Page 3 / 3

March 1, 2023, NASA ImaginAviation Watch Party UD-CCM and SAMPE UD Chapter will be hosting a NASA Watch Party. ImaginAviation is a virtual, free event to provide the community an opportunity to experience the latest innovations in NASA Aeronautics through the eyes of TACP'S University Innovation, Convergent Aeronautics Solutions, and the Transformational Tools and Technologies projects. In addition, this year's event will also include technology maturation and market infusion potential with support from industry, other government agencies, and NASA Aeronautic programs such as Advanced Air Vehicles, Airspace Operations and Safety, and Integrated Aviation Systems. Over 50 students from UD-CCM attended this event. *https://nari.arc.nasa.gov/imaginAviation/*

CCM CONNECTS: The Future Is Composites | Research Series, is annual research seminar series co-sponsored by our NASA ULI. The monthly series started in in April 2023 UD-CCM holds monthly sessions on various research projects, to date we have had a total of 14 presentations. The reviews are open to the public and attended by approximately 50 people (total of 700 attendees).

The reviews are open to the public typically included 3-4 talks. After the talks, a poster session with lunch is held in the lobby. The talks are recorded and posted on our CCM Capture Channel. Posted on website (presentations and videos) *https://www.ccm.udel.edu/research/research-reviews*

CCM CONNECTS: The Future Is Composites | Research Series

Spring / Summer Schedule – (40-50 attendees weekly)

April 4th	
Shagata Das, (Ph.D.C.E.) Graduate Student	Mechanical Behavior Of UV-Cured Composite Stepped Lap Adhesive Joints
Tania Lavaggi, (Ph.D.M.E.) Graduate Student	Vacuum Induced Preform Relaxation For The Manufacturing Of Thermoset Composites With Impermeable Interlayers
Alexander Legenstein, (Ph.D. Polymer Science) Graduate Student, Montanuniversität Leoben	Stretch Steering of Aligned Discontinuous Fiber Tapes on Highly Curved Paths Using Automated Fiber Placement
May 2nd	
Lukas Fuessel, (Ph.D.M.E.) Graduate Student	Influence of Deformation of Compliant Rollers on Tape Steering during Automated Tape Placement
Dr. Sagar M. Doshi Associate Scientist	Characterizing Adhesion of Polyimide PI Silica Composite Copper for Applications in Microelectronics
Professor Mark Mirotznik	Design of Multifunctional TuFF for Electromagnetic Applications
June 6th	
Colin Bonner, (Ph.D.E.C.E.) Graduate Student	The Additive Manufacturing of Conformal Electromagnetic Devices on Composite Substrates
Tekin Ozdemir, Ph.D. Postdoctoral Researcher	Polymer and Carbon Fiber Reclamation of Elium 188 O Infused TuFF Composites
Abhishek Bhesania Postdoctoral Researcher	Molecular Dynamics And Machine Learning Based Silane Chemistry Optimization For High Strain Rate Application

July 11th	
Dr. John Tierney Sr. Scientist	UD-CCM CDS Composite Design Software: Overview and Demonstrations
Dr. Pavel Simacek Research Associate III	Modeling Resin Infusion with LIMS
Dr. Bazle Z. Haque Sr. Scientist	Composite Damage Modeling with Rate Dependent Progressive Continuum Damage Model (rdpCDM) MAT162 in LS-DYNA
August 1st	
Branndon Chen, (Ph.D.M.S.E.) Graduate Student	Micro-Mechanical Investigation of Fiber Waviness Development in Carbon Fiber Thermoplastic Composite Processing
Theodore Fessaras, (Ph.D.E.C.E.) Graduate Student	Design and Additive Manufacture of Gradient Dielectrics for RF Devices
Nuwan Dewapriya Postdoctoral Researcher	Molecular Dynamics Investigation of the Effects of Defects and Transverse Pressure on the Axial Tensile Behaviors of Polyethylene Crystals and Fibrils

CCM host the Student Achievement Awards Day in May. This year 15 awardees were honored. Guest Speaker Dr. Steve McKnight, Director, Office of Energy Efficiency & Renewable Energy presented a talk on keys to a successful career in the composites industry, to students, staff, faculty, and external participants. The event was well attended (more than 60 participants) and provided valuable advice on professional development and career advancement. *https://www.ccm.udel.edu/education/student-achievements/*

Student Achievement Day 2023

May 4, 2023 – (55 attendees)

https://www.ccm.udel.edu/education/student-achievements/

R.L. McCullough Scholars Award	Faheem Muhammed, Ph.D.M.S.E.
Tsu-Wei Chou Composites Science and Innovation Award	Raja Ganesh, Ph.D.M.E. Dae Han Sung, Ph.D.M.E.
Achievement Award	Branndon Chen, (Ph.D.M.S.E.) Kaiyue Deng, (Ph.D.M.E.)
Progress Award	Tania Lavaggi, (Ph.D.M.E.) Sandra Milev, (Ph.D.C.E.)
Outstanding Senior Award	Aaron Fieger, MME Tommy Zhang, BME
Undergraduate Research Award	Alexander Barry Newark Charter High School
Visiting Researcher Award	Alexander Legenstein, Montanuniversität Leoben (Austria)
CCM Scholarship Award	Dr. Pavel Simacek
Directors' Award	Mr. Keith Carey Mrs. Corinne Hamed Mrs. Kristen Scully

Delaware Aerospace Education Foundation (DASEF) – UD Summer Camp 2023
Destination Moon – Space Beam Challenge on July 11th & 12th

SAMPE UD works in conjunction with the DASEF hosting thirty-two (32) students entering 7th, 8th and 9th grade attended UD Destination Moon summer camp. The camp integrates real world experiences with Lunar Studies, lessons in Development, Advanced Rocketry, Remote Sensing, Robotics, Computer Sim, Composite Materials & Telescope Building along with Field Trips. *https://dasef.org/aerospace/over_night.htm*

Delaware Aerospace Education Foundation – Destination Moon

July 12 & 13, 2023

https://dasef.org/aerospace/over_night.htm

Eligible for student entering 7th, 8th and 9th grade this camp integrates real world experiences with Lunar Studies, lessons in Crystal Development, Advanced Rocketry, Remote Sensing, Robotics, Computer Sim, Composite Materials & Telescope Building & Field Trips.

This year's challenge was manufacturing and testing a SPACE BEAM.
32 student attended
July 12 – Composite Center Tour
July 13 – Space Beams: Design, Build, Test, Results






Summer

Research Symposium on August 11th, 2023, with over 50 attendees. The symposium included 28 students (short presentations and poster sessions) from UD-CCM including 3 from local high schools. *https://www.ccm.udel.edu/research/summer-research-posters/*

Summer Symposium

August 11, 2023 – 35 presenters from high school to Ph.D., over 50 in person attendance expected

2023 Participants

STUDENT	Level/Title
Bakshi, Kayshavi	
Barry, Alexander James	High School
Benvenuto, Matthew	Research Intern
Blackburn, Logan Nicholas	HComp.E-Fr.
Bogetti, Eli	ME-Sr. 4+1
Breder, Richard	ECE-So
Brown, Andrew Thomas	ME-Sr.
Carroll, Christina JoAnn	ECE-Sr.
Conklin, Abigail	CHE-So
Duncan, Nicholas Anthony	ME-So
Ferrone, Owen	HME-Jr.
Ghin, Steffan	
Gong, Wiley Jia-Wei	
Guillen Kuroki, Jiro Guillermo	CHE-Jr.
Haiko, Elyas Andrew	ME-4+1
Hausler, Justin	UPITT ME-Sr.
Higazi, Adam Walid	CPEG-So.

STUDENT	LEVEL/TITLE
Marquard, Hayden	CHE-Jr.
Martin, Robert	ME-Jr
McKnight, Erin Simone	CHE-Jr.
Mirotznik, Benjamin M	HCHE-So.
Mukherjee, Iveena Avighna	High School
Ogbuanu, Kelechi Okechukwu	PhD
Phommachanh, Tyler	ME-Sr
Rao, Nathan	High School
Reddy, Suraj	High School
Riehl, Nathaniel	CE-Sr.
Rock, Elizabeth Rose	CHE-Jr.
Skourlis, Gerard Alexander	CHE-Fr
Tallman, James Francis	Cornell Univ.
Tetteh, Obed	Southern Univ.
Whealton, Charles Tong	HME-So
Wierzbicki, Jared Jonathan	HBio-Fr
Yezek, Matthew	ME-So.
Young, Matthew David	HME-So

Southern University Education/Workforce Training and Outreach Activities

In year-three of the TuFF ULI project, Southern University engaged in several education/workforce training and outreach initiatives by leveraging SU's CREST Center for Multifunctional Composites education and outreach program activities for underrepresented minorities. The activities are listed in Table 1 below. Seven events at eight middle schools in East

Baton Rouge, LA were held starting in September 2022 through March 2023. The events engaged more than 1700 URM to STEM field and provided widespread exposure to NASA and industry interests.

K-12 Outreach **Southern University and A&M College, College of Sciences and Engineering**				
Date of Activity	**Name of School / Program**	**Parish**	**Grades of Participants**	**Number of Students**
09/02/2022	Westdale Middle School	East Baton Rouge	7^{th} and 8^{th} grades	75
09/16/2022	Woodlawn Middle School	East Baton Rouge	7^{th} and 8^{th} grades	66
10/14/2022	Istrouma Middle School	East Baton Rouge	7^{th} and 8^{th} grades	44
10/28/2022	Scotlandville Middle Pre-Engineering Academy	East Baton Rouge	7^{th} and 8^{th} grades	37
11/11/2022	Sherwood Middle Academic Magnet School	East Baton Rouge	7^{th} and 8^{th} grades	34
03/23/2023	East Baton Rouge – 7^{th} Grade Day • Westdale Middle School • Northdale Academy • Southeast Middle School • Mayfair Laboratory • Glasgow Middle School	East Baton Rouge	7^{th} grade	• 235 • 12 • 321 • 49 • 163
03/30/2023	East Baton Rouge – 7^{th} Grade Day	East Baton Rouge	7^{th} grade	

Overall, faculty and students participated in seven outreach activities. Figure 1 shows some highlights of four of these activities. In Figure 1 from top left to right and bottom left to right *a) Capitol Middle School b) Westdale Middle School c) Sherwood Middle School d) Scotlandville Middle School.*

.

Education/workforce training and outreach initiatives at Southern University

SU students supported with TuFF ULI funds participated in CREST Center sponsored research education for undergraduate (REU) during fall 2022, spring 2023 semester and in person summer REU programs. Activities included: i) REU projects with graduate student and professors as mentors, ii) weekly virtual and in person professional development seminars with invited guest presenters, iii) Tours and training in SU and Louisiana State

SU Faculty and students attending ERN, February 2023

University (LSU) laboratories, iv) With travel support from TuFF ULI six undergraduate (3) and graduate (3) students attended and participated in the National Science Foundation Emerging Researchers National Conference (ERN) in Washington DC, February 2023. The students participated in poster and oral presentations competitions. Figure 2 shows SU ERN delegation. Tuff ULI funding was also used to support SU REU and graduate students to attend 2023 Diversity in STEM Conference this summer organized by NSF funded LS PACS Models in New Orleans, LA in July 2023. Students and faculty in attendance are shown below.

Group Picture of SU REU and Graduate Students in attendance at Group (left) and SU REU students (right)

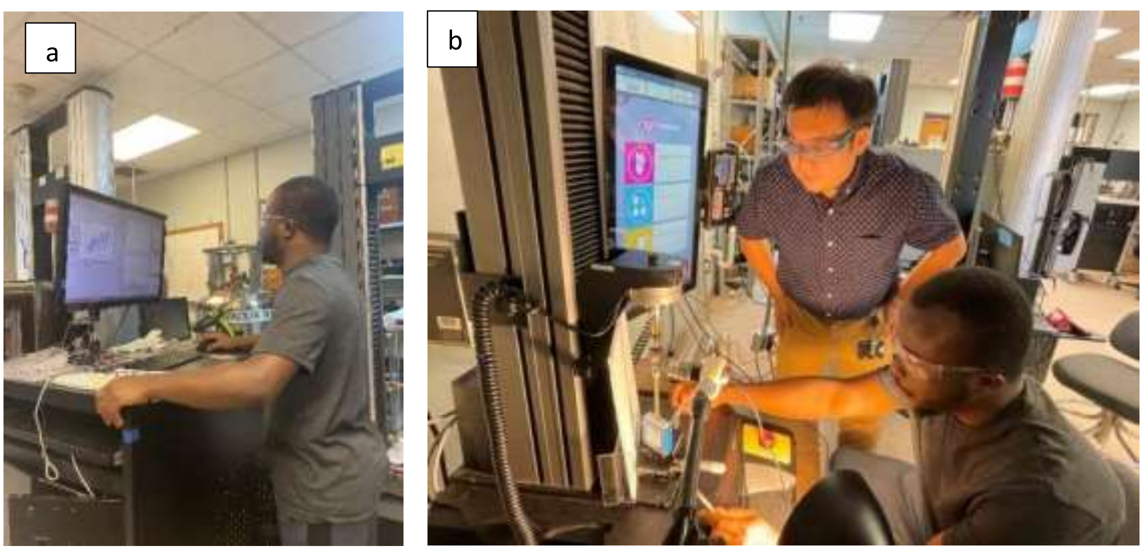

SU Graduate student Obed Tetteh UD student Taka Kubota conducting experiments at CCM Lab on self-healing interphases using vitrimer polymers.

Diversity Data: September 2022 – August 2023

Total Number of PI/Co-I's: 14

- Male: 14 (100%)
- Female: 0 (0%)
- URM: 2 (14%)

Total Number of Universities: 2

Total Number of Industry Partners: 3

Total Number of Students: 81

- Male: 67 (83%)
- Female: 14 (17%)
- ULI Funded: 18
- ULI Unfunded: 61
- Graduate: 21
- Undergraduate: 58
- URM: 13 (21%)
- Postdocs: 2

Other Support Staff: 14

- Male: 7 (50%)
- Female: 7 (50%)

Schedule and Milestones

The program milestones and scheduled are shown below for the 4-year program.